

Cassini Ultraviolet Imaging Spectrograph

Ring Solar Occultation Atlas Volume 1: Revs 009 - 090

Version: 1.0
June 18, 2018

Table of Contents

The table lists all solar occultations observed by UVIS over the course of the Cassini mission. The table includes the rev number, whether the occultation was ingress or egress, the radial range sampled in the ring plane, the instrument integration period, solar elevation angle of the occultation, and duration of the occultation.

For each occultation there are four graphical products: (1) a plot of the total signal collected as a function of ring plane radius (the data have been binned spectrally); (2) the nominal radial resolution as a function of ring plane radius; (3) the azimuthal look angle as a function of ring plane radius; (4) a geometric rendering of Saturn from the point of view of Cassini at the temporal midpoint of the occultation. The nominal radial resolution does not include effects due to the nonzero angular dimensions of the Sun, diffraction, or smearing. The geometric rendering includes the UVIS EUV Solar occultation window field of view.

Occultations are presented chronologically in the order they were observed. In order to keep the file sizes small, the atlas is divided into volumes.

Introduction

The Cassini UVIS Extreme Ultraviolet Channel (EUV) had a solar port offset 20 degrees from the main UVIS optical axis to allow safe solar viewing. This was co-aligned with the Visual and Infrared Mapping Spectrometer (VIMS) solar port so that both instruments could observe the Sun simultaneously. Solar occultations by Saturn's atmosphere, Titan's atmosphere, the plumes of Enceladus, and Saturn's rings were observed. Because of the finite angular size of the solar disk projected onto the rings as seen from Cassini and longer integration times, the nominal spatial resolution of the ring solar occultations is much worse than that of the stellar occultations.

On the first ring solar occultation on "rev 9" it was discovered that an offset between the VIMS and UVIS solar fields of view resulted in the Sun falling just at the edge of the UVIS field of view when the VIMS solar boresight was pointed at the Sun. This resulted in an unusual occultation profile for rev 9 that also, coincidentally, passed near a particularly dust region of the F ring, resulting in a prominent diffraction signal (Becker et al. 2018). Most future occultations used UVIS pointing because that enabled both VIMS and UVIS to see the full solar disk due to the differences in instrument field of view shapes and sizes. The misalignment of rev 9 was approximately re-produced on the solar occultations on revs 90, 172 and 181.

Description of Data Products in the Atlas

The data are shown summed in the spectral dimension and plotted as a function of nominal ring plane intercept of the line of sight to the Sun. The data plots are at the full temporal resolution recorded. The summary table identifies the integration period for each occultation.

Two additional geometry plots are included for each occultation: (1) the radial ring plane resolution of the occultation (in the frame of Saturn, not accounting for ring particle motion, size of the solar disk, or diffraction); and (2) the value of ϕ , an angle measured in the ring plane in the counterclockwise sense from the outward radial vector at the measurement point to the direction to the Sun projected into the ring plane. Thus, an observation where the look vector to the Sun is tangent to the rings has $\phi=90$ degrees.

On the page following the data plots, a geometry visualization is shown at a time near the middle of the occultation. The position of the UVIS EUV solar port field of view is labeled on each of these plots. Occultations that cut a chord across the rings, are presented here as separate "Ingress" and "Egress" occultations, referring to the portion of the occultation where the observation point is approaching or receding from Saturn, respectively.

Document assembled by Joshua Colwell, UVIS Co-Investigator, University of Central Florida, with the assistance of Tina Notrika, UCF.

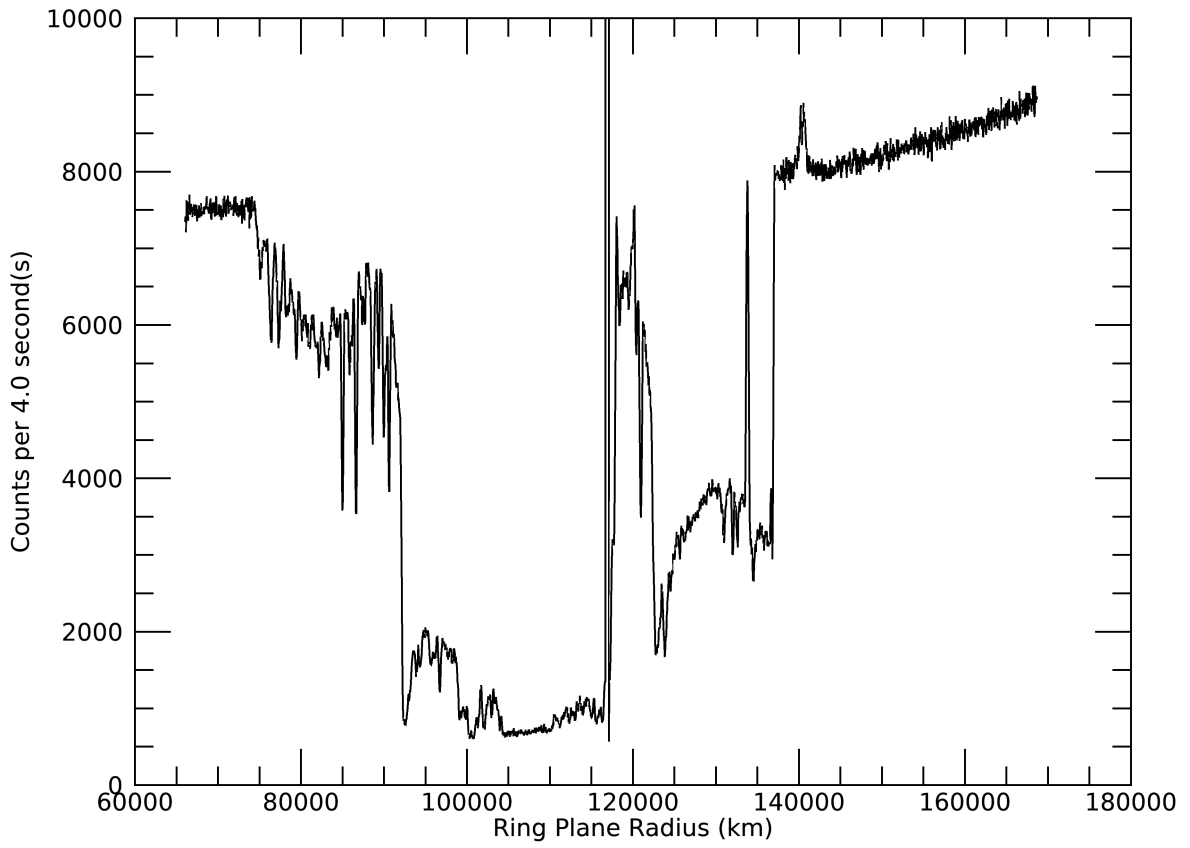
References

1. Becker, T. M., J. E. Colwell, L. W. Esposito, N. O. Attree, C. D. Murray 2018. Cassini UVIS Solar Occultations by Saturn's F Ring and the Detection of Collision-Produced Micron-Sized Dust. *Icarus* **306**, 171-199, doi:10.1016/j.icarus.2018.02.006.
2. Esposito, L. W., J. E. Colwell, and W. E. McClintock 1998. Cassini UVIS Observations of Saturn's Rings. *Planet. Space Sci.* **46**, 1221-1235.
3. Esposito, L. W., C. A. Barth, J. E. Colwell, G. M. Lawrence, W. E. McClintock, A. I. F. Stewart, H. U. Keller, A. Korth, H. Lauche, M. Festou, A. L. Lane, C. J. Hansen, J. N. Maki, R. A. West, H. Jahn, R. Reulke, K. Warlich, D. E. Shemansky, and Y. L. Yung 2004. The Cassini Ultraviolet Imaging Spectrograph Investigation. *Space Sci. Rev.* **115**, 299-361.

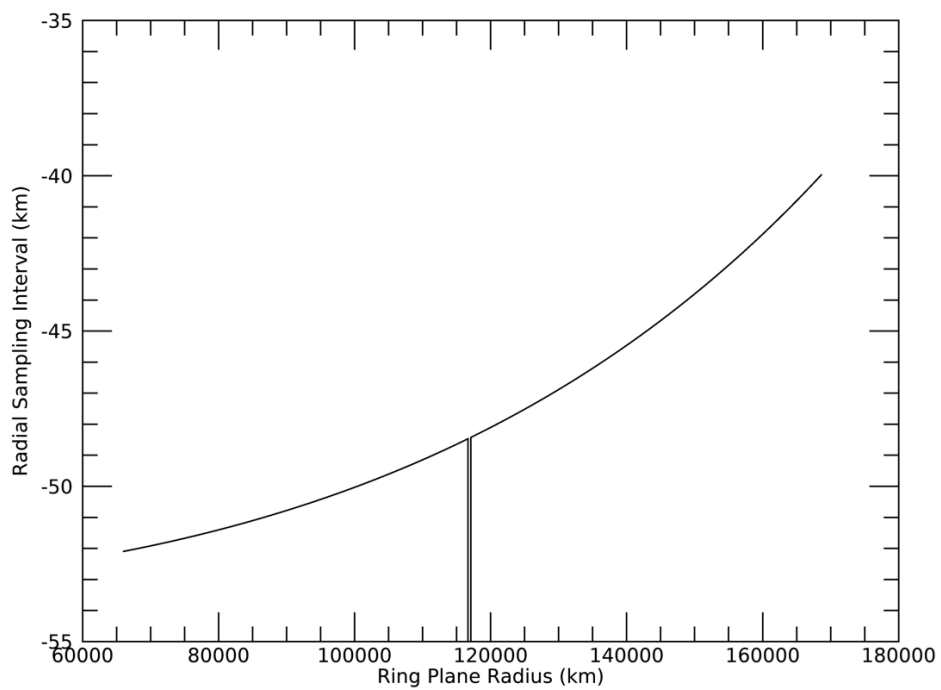
Rev	Ing/Eg	Year/Day	B0	ϕ (degrees)	Radius (km)	Int. Period (s)	Duration (minutes)	I0 (counts/int.)	Background (counts/int.)
9	I	2005-159	-21.45	281.96-281.67	168,669-66,033	4	144.5	8.0E+03	6.0E+02
11	I	2005-196	-21.07	284.83-286.18	116,000-53,978	4	81.7	4.0E+05	1.0E+03
28	I	2006-257	-15.86	281.20-230.96	128,084-87,624	37	633.9	2.5E+06	4.0E+03
28	E	2006-258	-15.86	234.16-230.96	87,490-87,624	37	31.4	2.5E+06	4.0E+03
43	I	2007-114	-12.76	41.24-78.81	126,232-100,226	5.5	38.8	4.7E+05	4.0E+02
43	E	2007-114	-12.76	78.81-139.77	100,226-205,453	5.5	129.4	4.7E+05	6.0E+02
55	I	2008-003	-9	314.11-258.18	172,488-96,962	4	40.1	3.2E+05	8.0E+02
55	E	2008-003	-9	258.18-207.70	96,962-151,727	4	73	3.2E+05	1.0E+03
59	I	2008-051	-8.27	331.78-262.26	194,733-68,372	4	34.3	3.2E+05	1.2E+04
59	E	2008-051	-8.27	262.26-257.22	68,372-68,628	4	1.1	3.2E+05	1.2E+04
62	I	2008-083	-7.79	337.93-264.72	257,380-74,524	4	41.7	3.2E+05	2.1E+03
62	E	2008-083	-7.79	264.72-192.75	74,524-238,015	4	38.3	3.2E+05	2.1E+03
65	I	2008-111	-7.36	332.21-266.13	206,054-83,837	1	30.2	8.1E+04	1.0E+02
65	E	2008-111	-7.36	266.13-194.65	83,837-262,873	1	40	8.1E+04	1.5E+02
66	I	2008-121	-7.21	337.36-266.20	261,953-85,115	1	38.9	7.8E+04	5.5E+02
66	E	2008-121	-7.21	266.20-194.49	85,115-270,107	1	40.2	7.8E+04	7.0E+02
90	I	2008-298	-4.49	346.51-268.82	445,890-95,719	2	36.3	4.0E+03	Unknown
90	E	2008-298	-4.49	268.82-206.69	95,719-204,613	2	15	4.3E+03	Unknown
172	I	2012-267	15.9	320.48-308.40	150,286-78,637	1	70.1	4.0E+03	6.0E+01
181	E	2013-044	17.5	147.36-153.60	100,304-148,010	1	35.3	1.8E+03	6.0E+01
239	I	2016-221	26.4	348.95-254.61	157,454-119,150	2	59.1	1.5E+05	1.0E+02
239	E	2016-221	26.4	103.36-134.95	59,983-150,709	2	151.6	1.5E+05	4.0E+02
241	I	2016-245	26.5	4.58-64.53	161,762-81,459	2	212.4	1.5E+05	1.0E+02
241	E	2016-245	26.5	64.53-116.75	81,459-132,557	2	158.7	Unknown	4.0E+02
243	I	2016-269	26.5	53.17-65.08	71,084-69,558	2	22.1	1.4E+05	Unknown
243	E	2016-269	26.5	65.08-119.41	69,558-118,986	2	146	1.4E+05	4.0E+02
245	I	2016-288	26.5	16.56-66.62	147,966-95,457	2	181.5	1.4E+05	4.0E+02
245	E	2016-288	26.5	66.62-82.74	95,457-99,340	2	44.1	Unknown	Unknown
249	I	2016-325	26.6	17.64-67.75	148,772-96,097	1	194.8	5.1E+04	1.0E+02
249	E	2016-325	26.6	67.75-117.77	96,097-148,630	1	194.3	5.1E+04	1.0E+02
254	I	2016-361	26.6	11.24-69.07	146,194-78,903	1	221.3	6.5E+04	1.5E+02

254	E	2016-361	26.6	69.07-126.58	78,903-145,372	1	218.9	6.5E+04	2.0E+02
257	I	2017-017	26.7	6.64-16.07	145,205-111,292	1	71.6	6.5E+04	Unknown
261	E	2017-046	26.7	118.88-143.42	68,714-147,371	1	159.6	6.5E+04	2.0E+02
263	E	2017-060	26.7	133.09-143.50	75,268-113,102	1	73.6	Unknown	2.0E+02
265	E	2017-074	26.7	146.20-152.35	95,650-147,462	1	95.1	6.4E+04	2.0E+02
267	E	2017-089	26.7	152.28-156.80	95,293-153,775	1	105.6	6.6E+04	2.0E+02
269	I	2017-103	26.7	348.26-349.55	157,777-117,823	1	72.1	6.4E+04	Unknown
271	E	2017-116	26.7	171.30-169.90	126,863-174,743	1	87.1	6.7E+04	Unknown
279	I	2017-168	26.7	321.49-267.36	127,778-77,483	1	180.1	Unknown	1.0E+02
279	E	2017-168	26.7	267.36-214.41	77,483-126,099	1	173.8	Unknown	1.0E+02

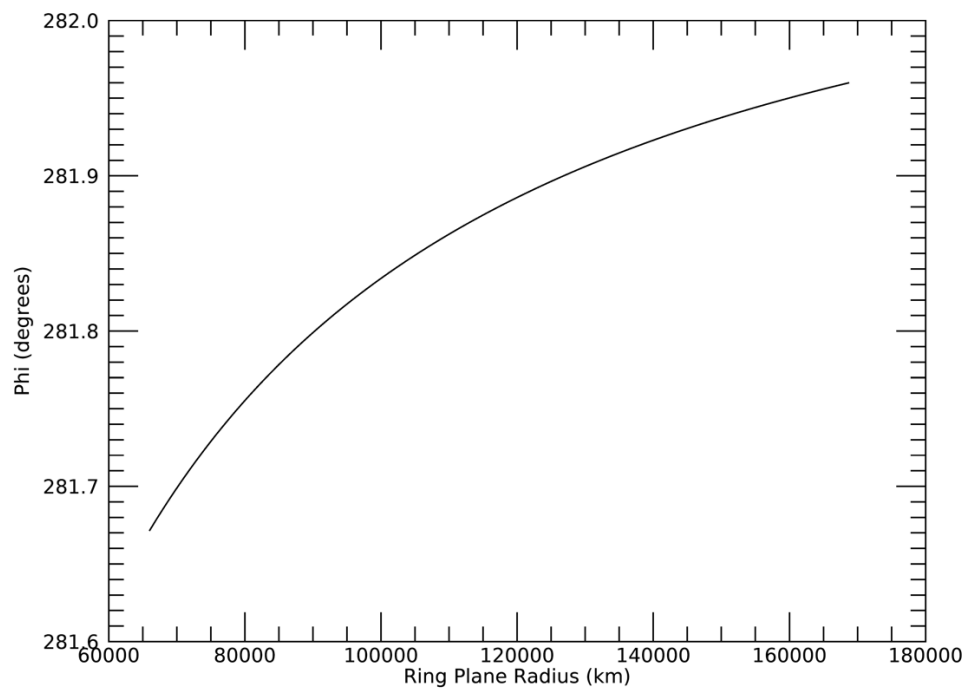
Rev 9I Signal

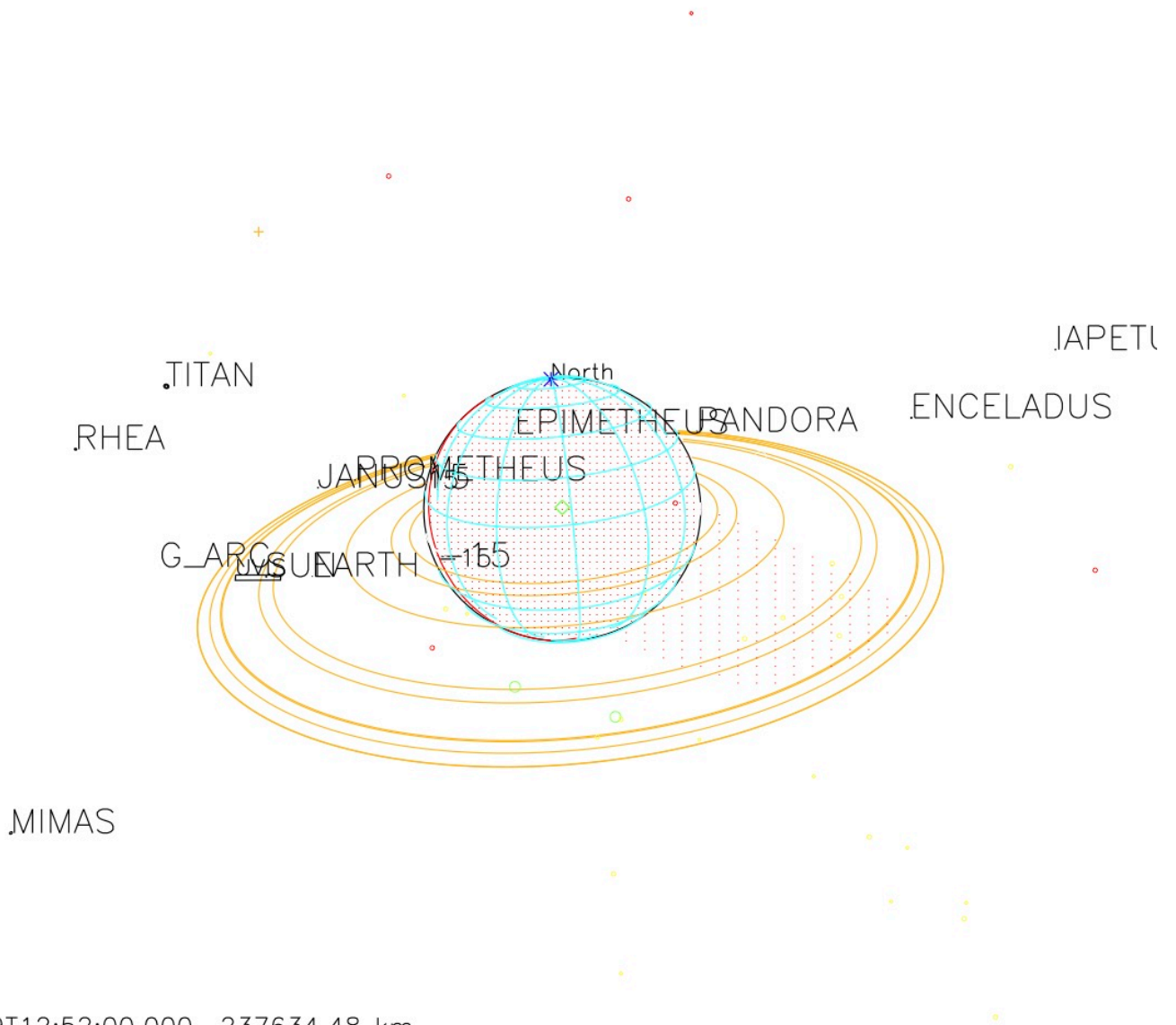


Rev 9I Radial Resolution



Rev 9I Phi





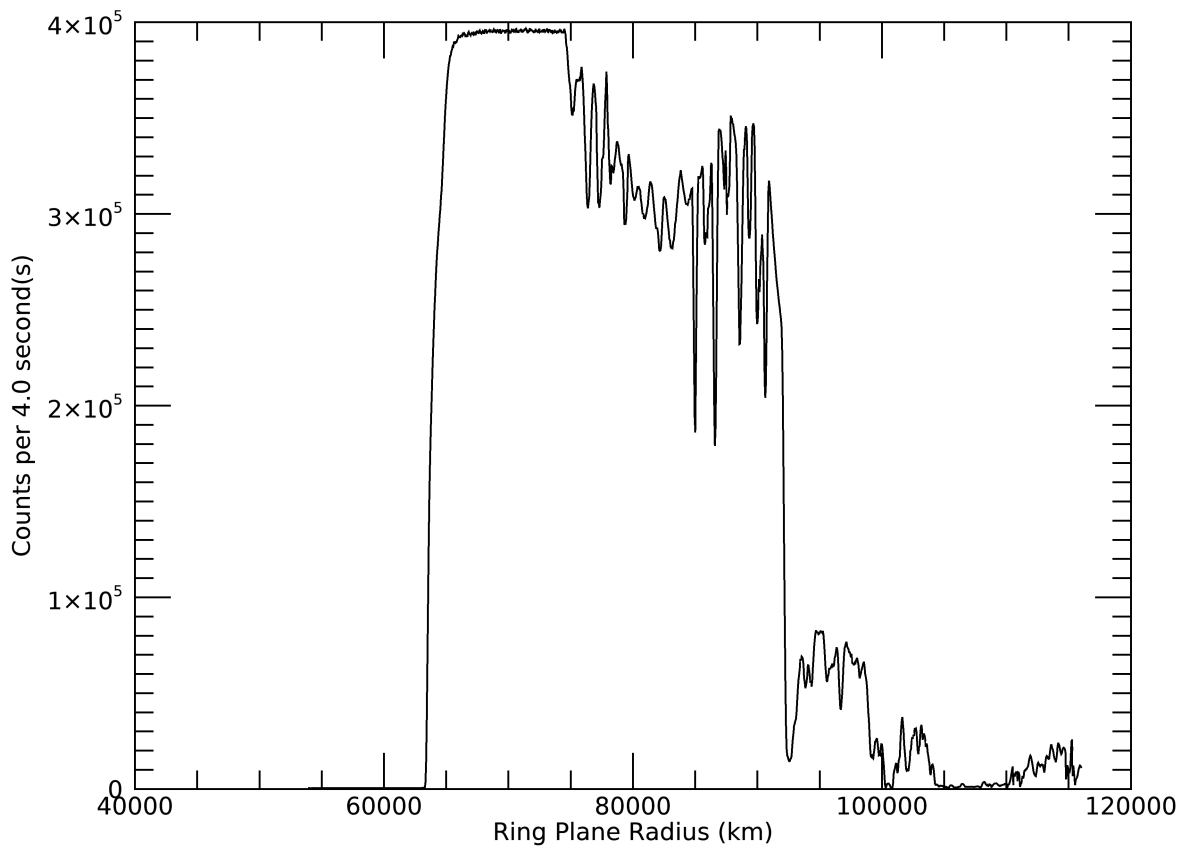
2005-159T12:52:00.000 237634.48 km

Target RA/dec: 270.14, -16.54 ◊

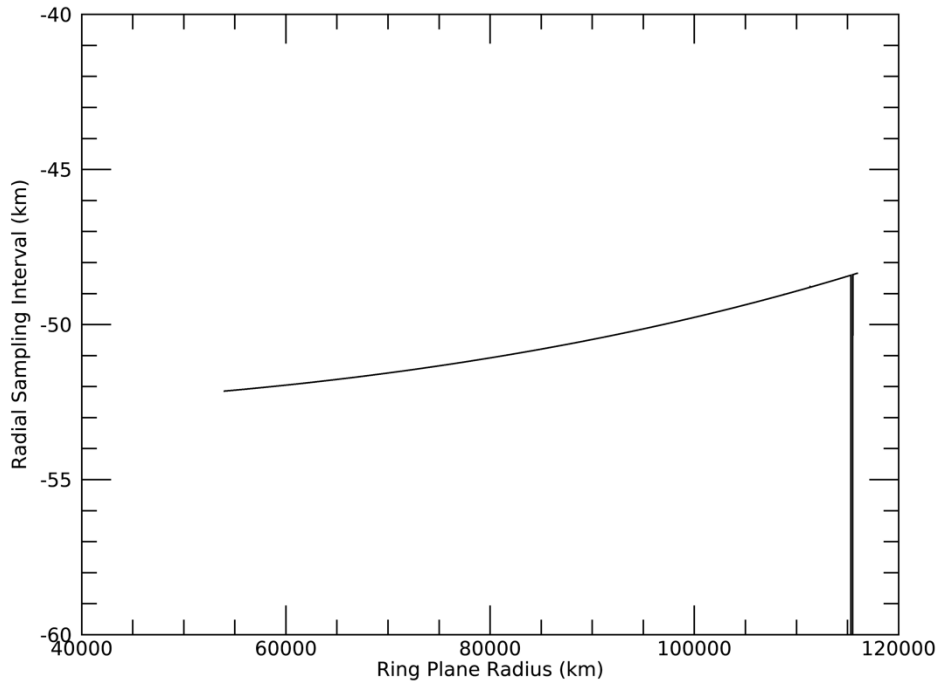
Subsolar lat/lon: -17.73, -121.40

Sub-s/c lat/lon: 17.85, 26.57

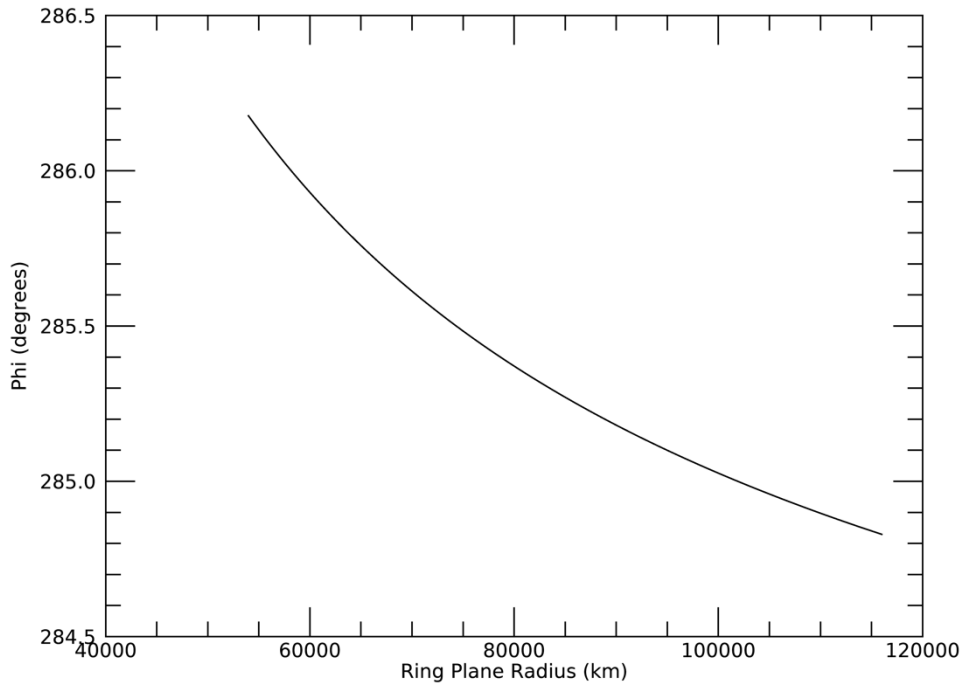
Rev 11I Signal

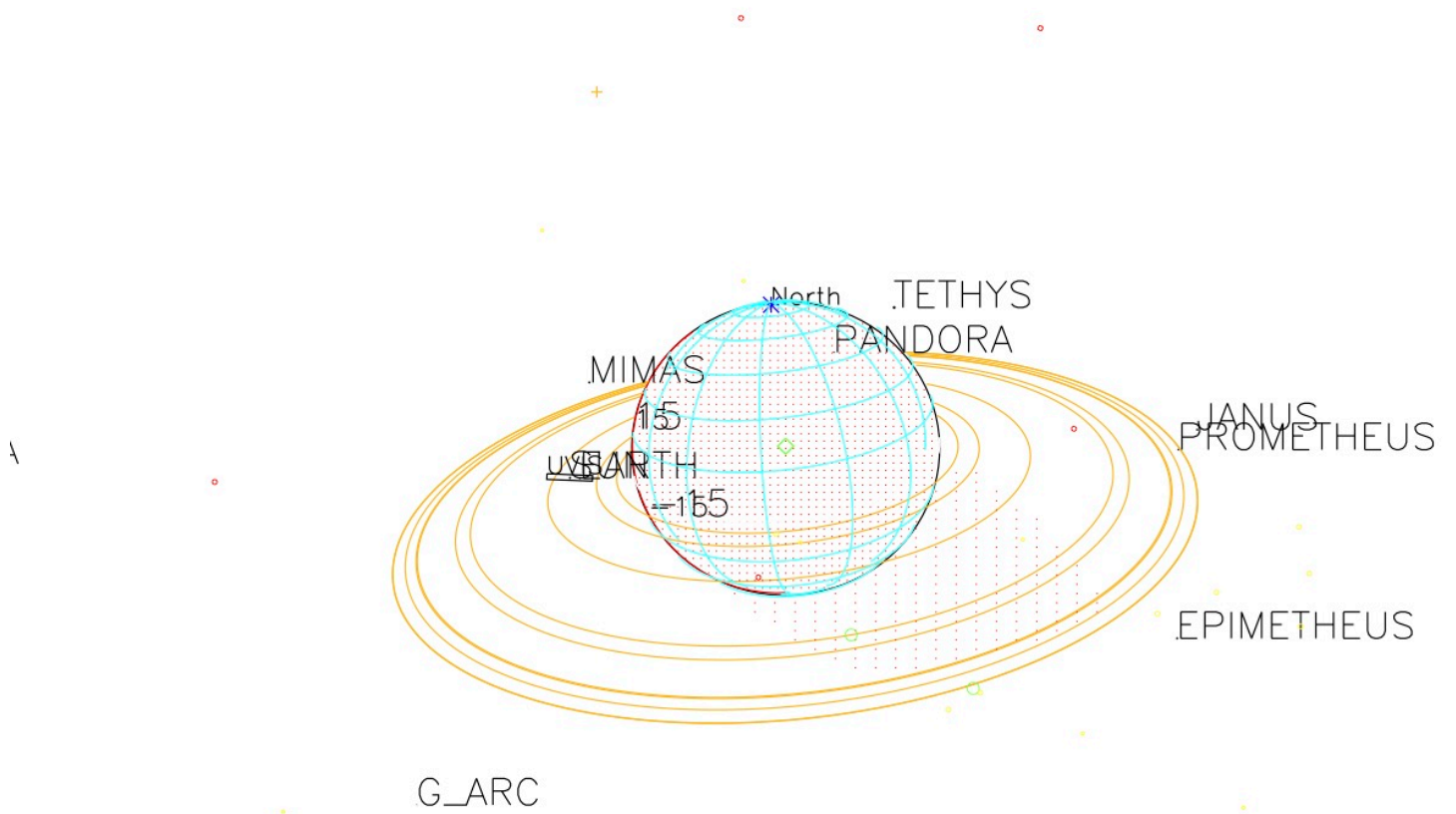


Rev 11I Radial Resolution



Rev 11I Phi





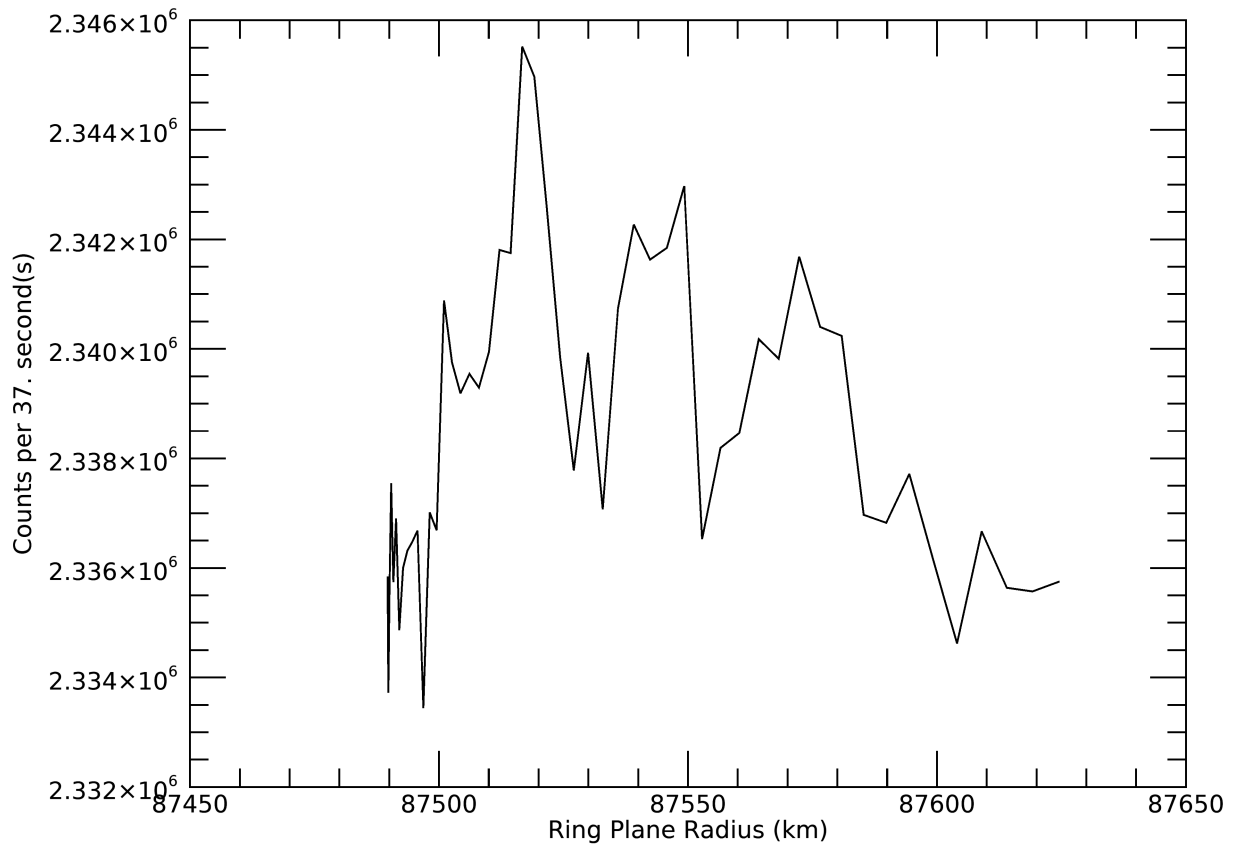
2005-196T01:22:00.000 257021.82 km

Target RA/dec: 282.88, -18.79

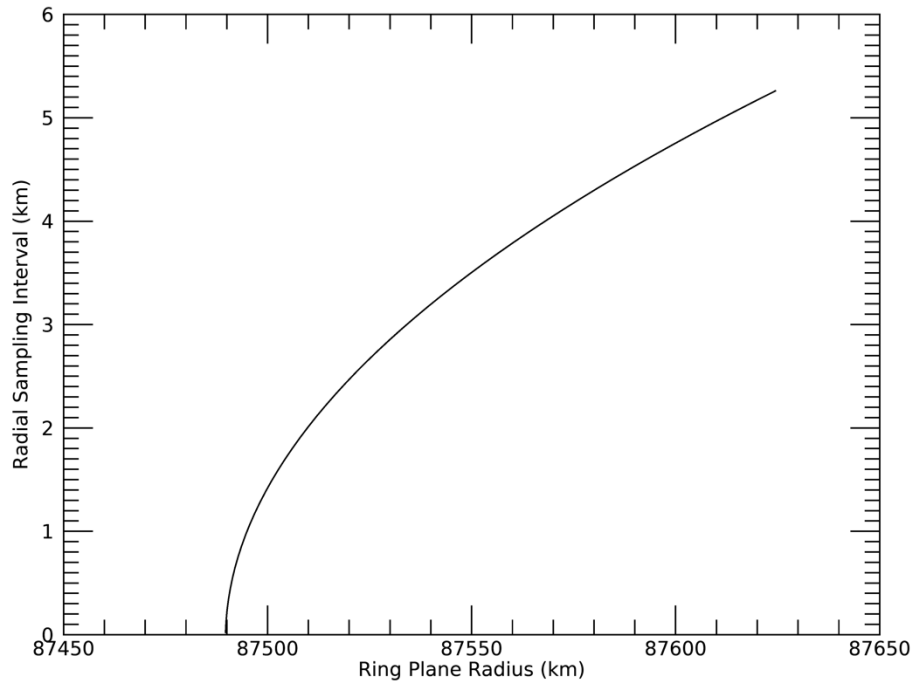
Subsolar lat/lon: -17.40, 149.12

Sub-s/c lat/lon: 18.70, -51.11

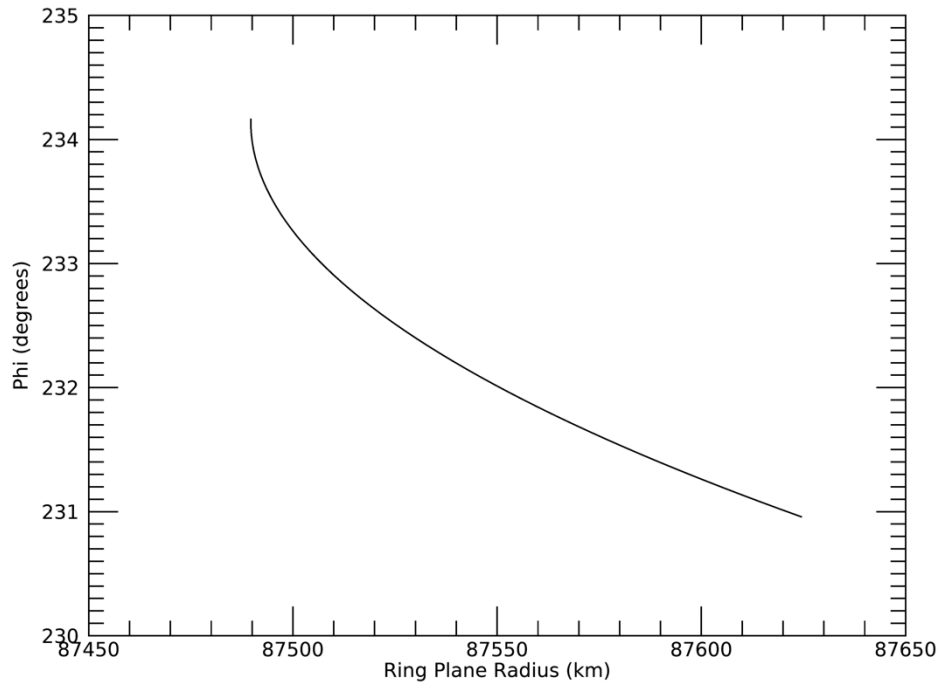
Rev 28E Signal

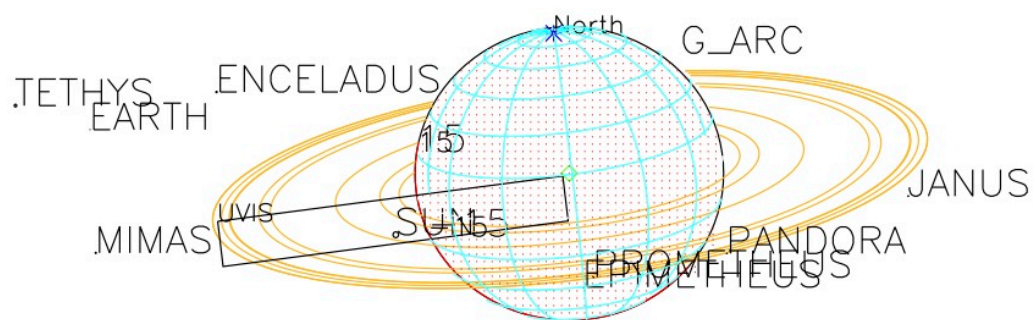


Rev 28E Radial Resolution



Rev 28E Phi





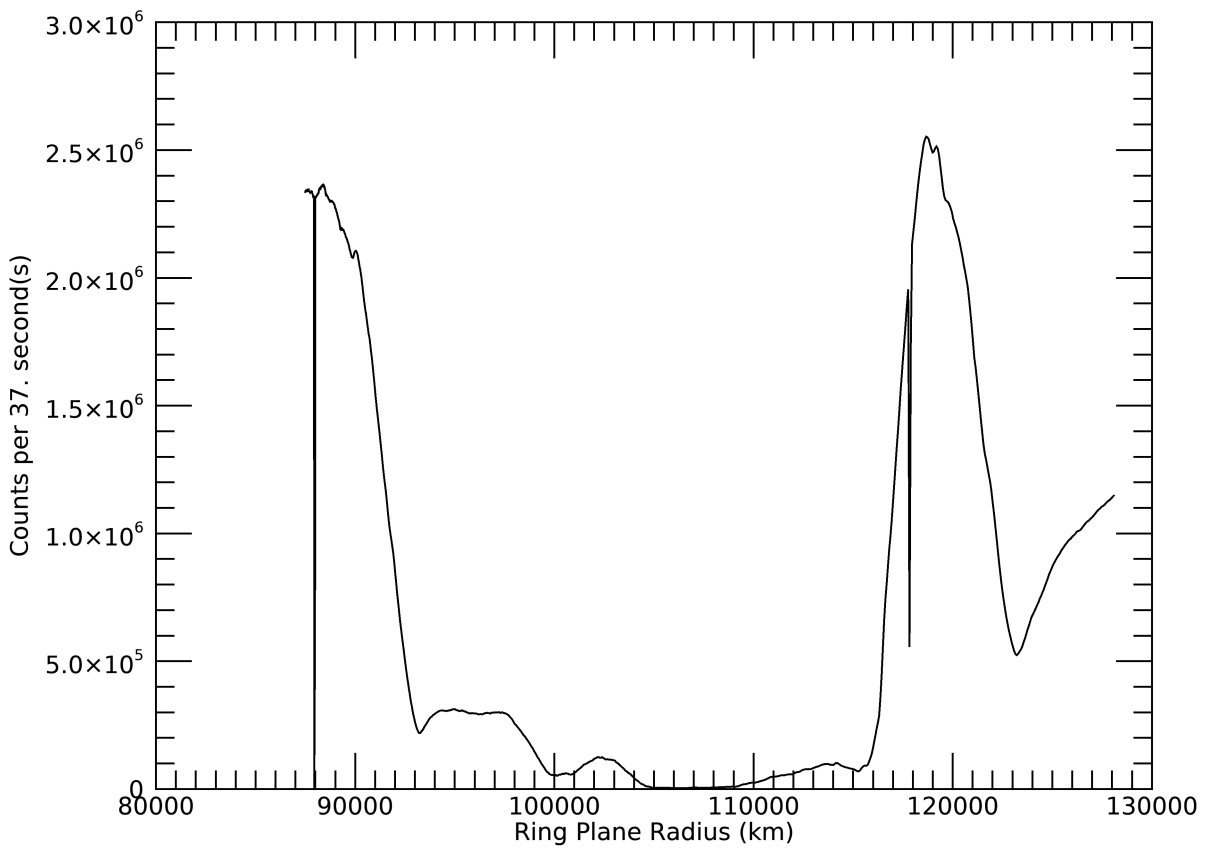
2006-258T05:57:00.000 2120453.5 km

Target RA/dec: 317.01, -16.29

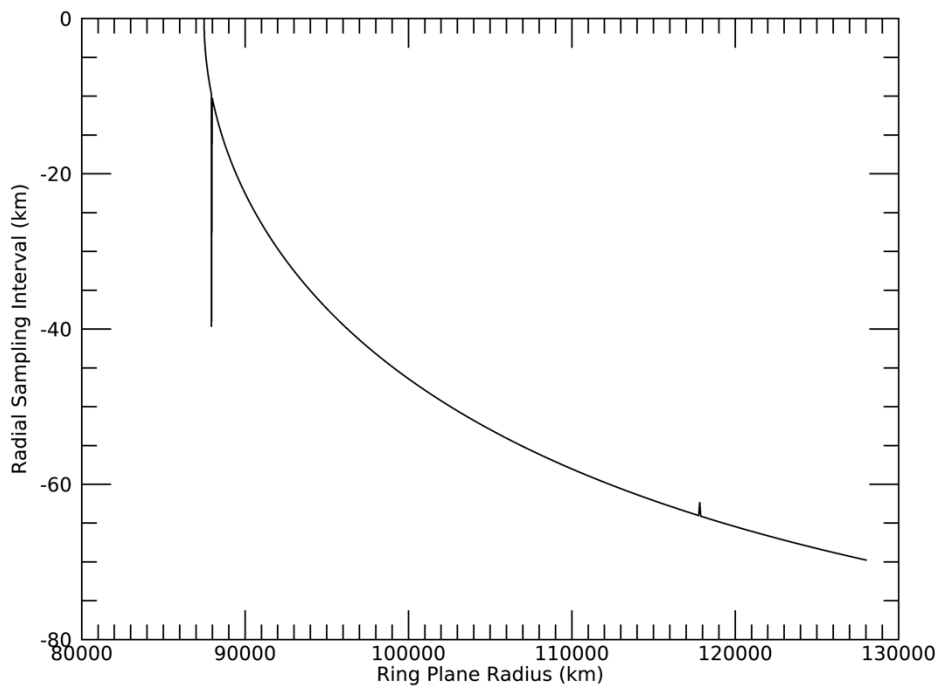
Subsolar lat/lon: -13.01, 120.90

Sub-s/c lat/lon: 12.75, -61.07

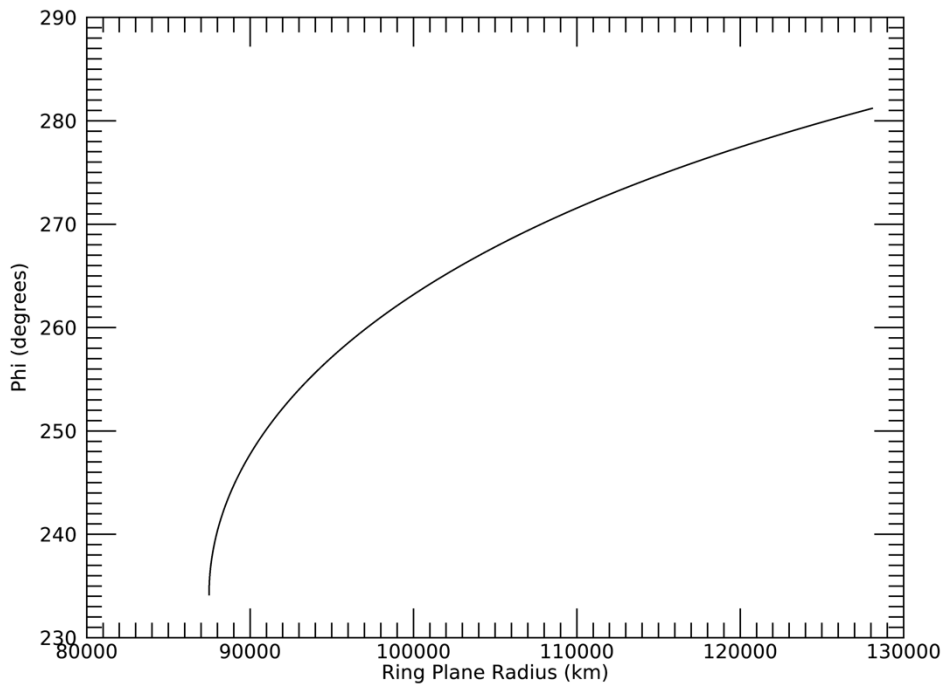
Rev 28I Signal



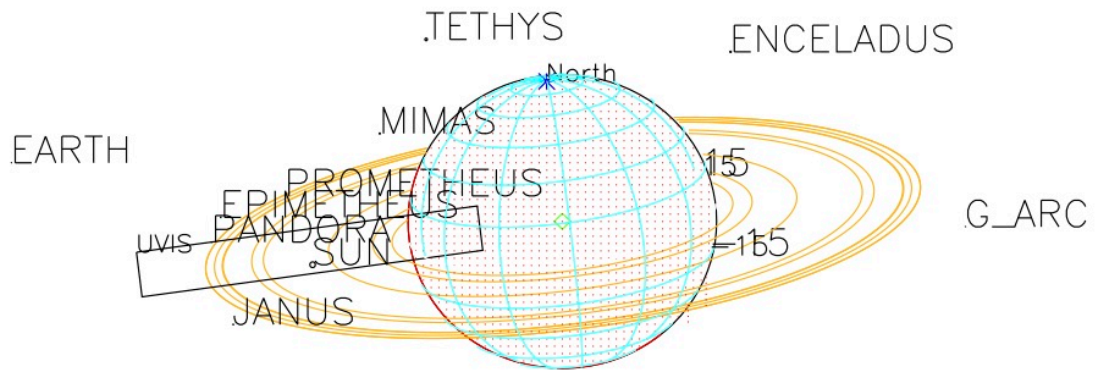
Rev 28I Radial Resolution



Rev 28I Phi



TITAN



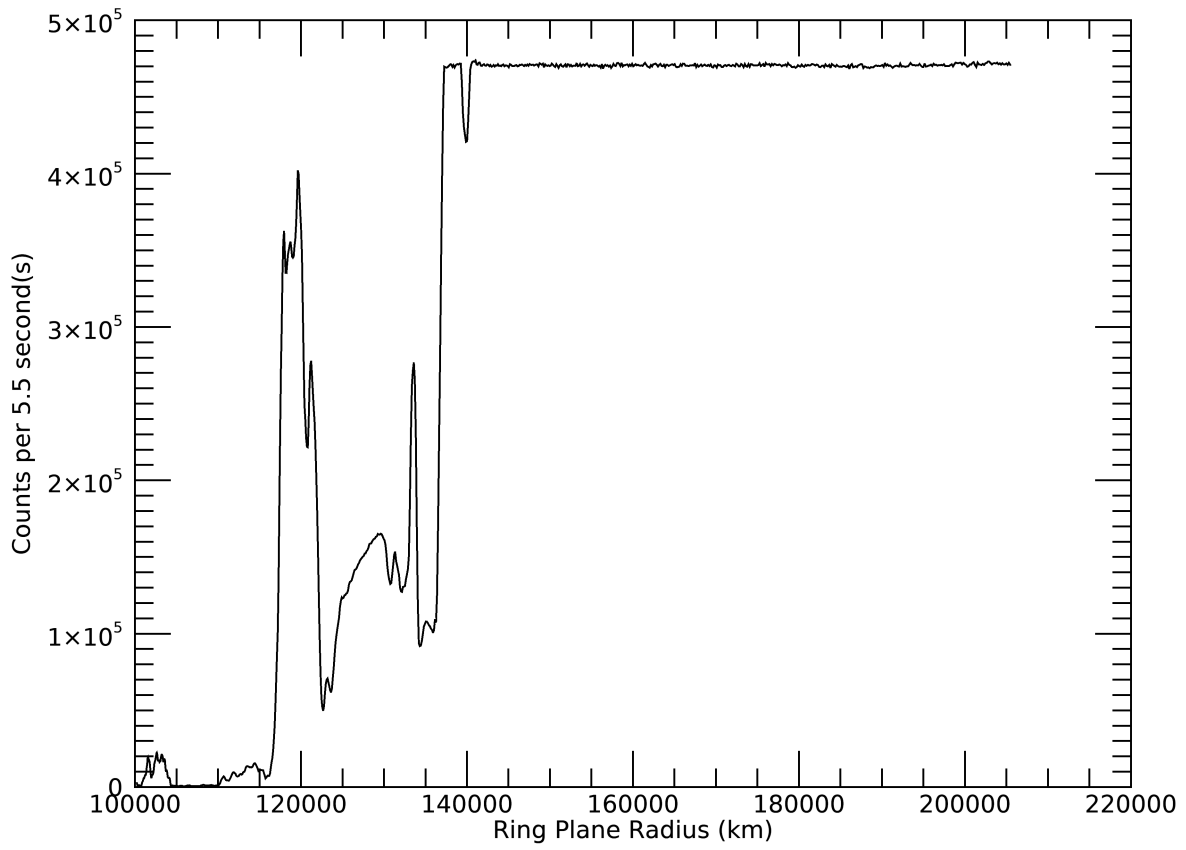
2006-258T00:39:00.000 2092433.2 km

Target RA/dec: 316.12, -16.48

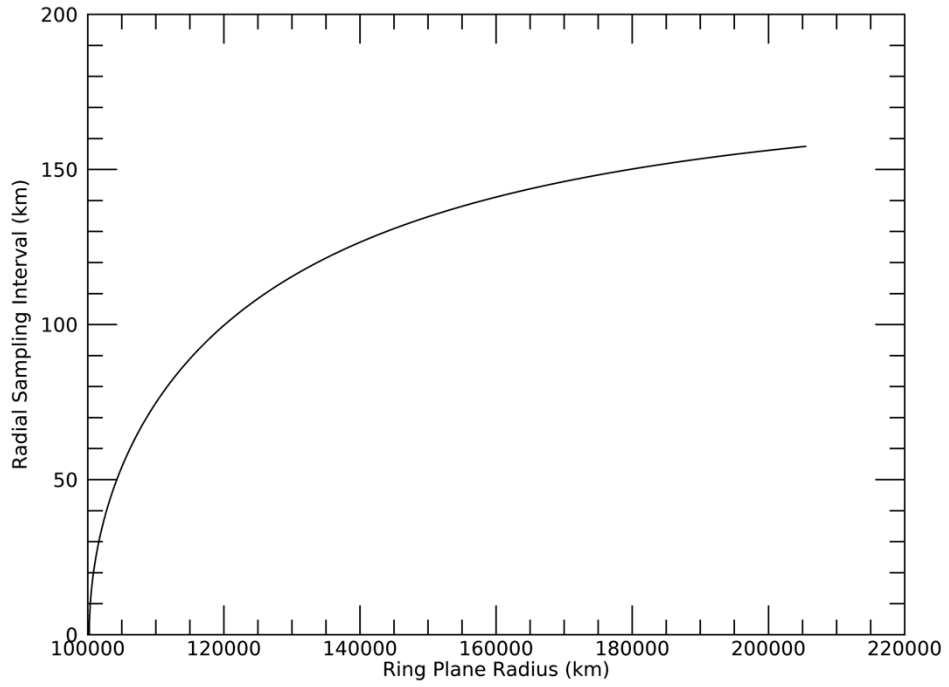
Subsolar lat/lon: -13.02, -60.06

Sub-s/c lat/lon: 12.99, 117.13

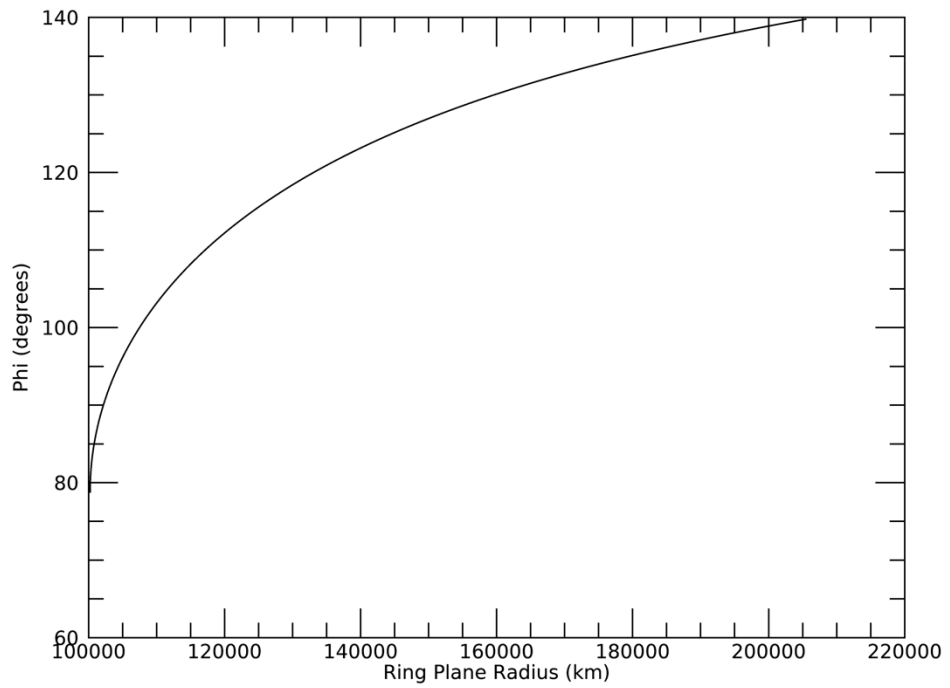
Rev 43E Signal

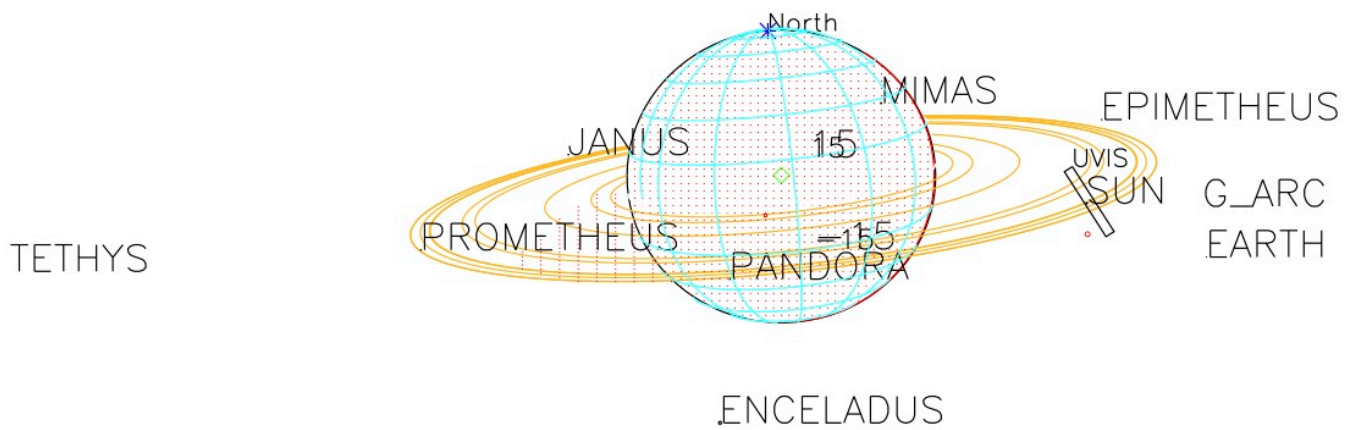


Rev 43E Radial Resolution



Rev 43E Phi





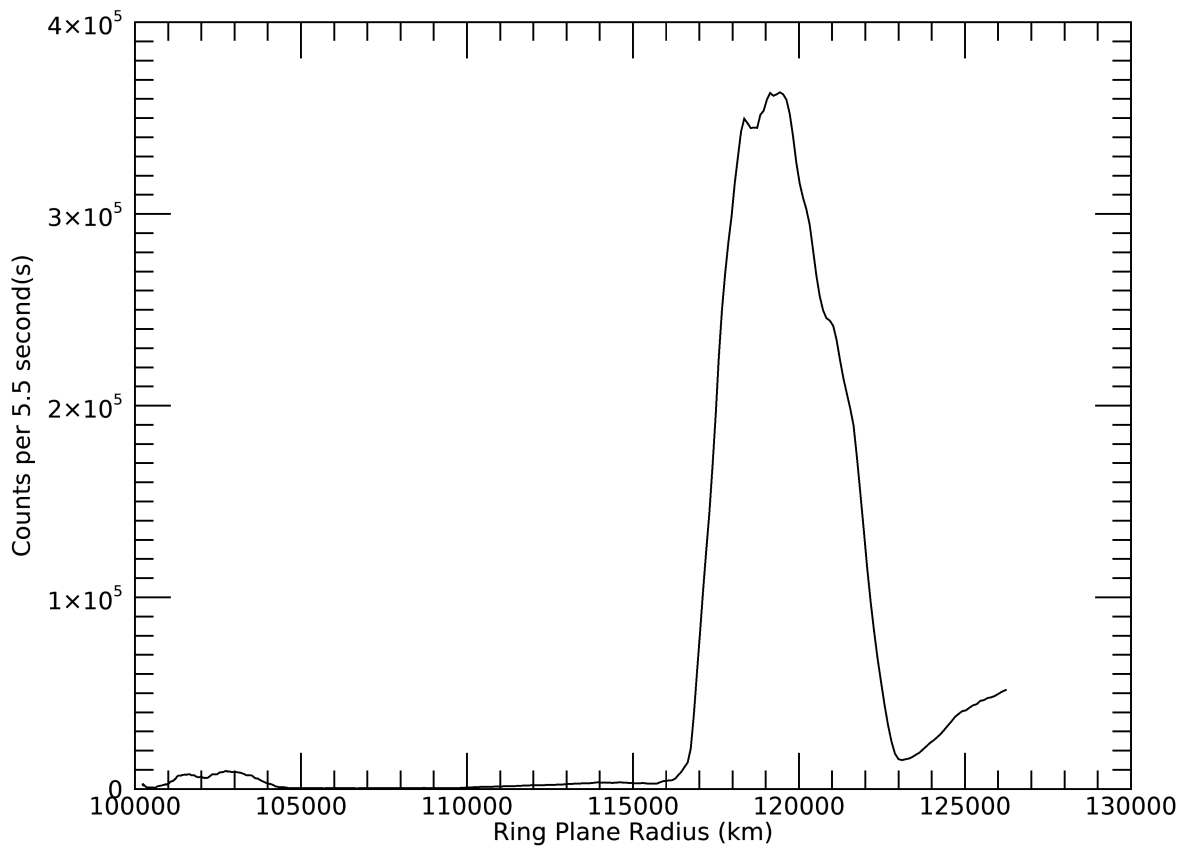
2007-114T11:22:00.000 437730.47 km

Target RA/dec: 342.81, -13.84

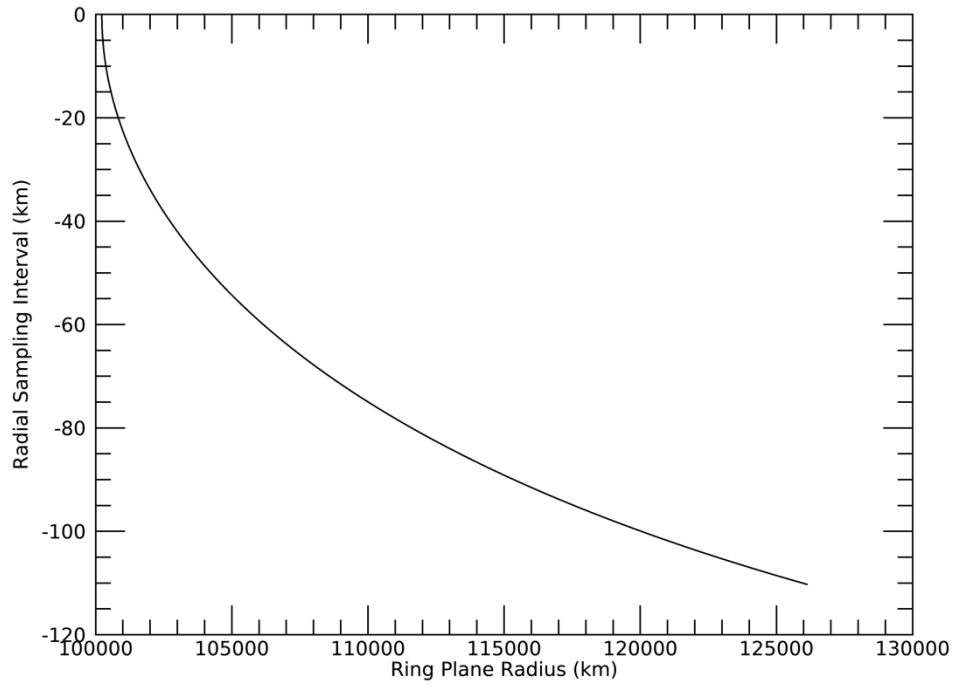
Subsolar lat/lon: -10.44, 40.00

Sub-s/c lat/lon: 8.66, -124.43

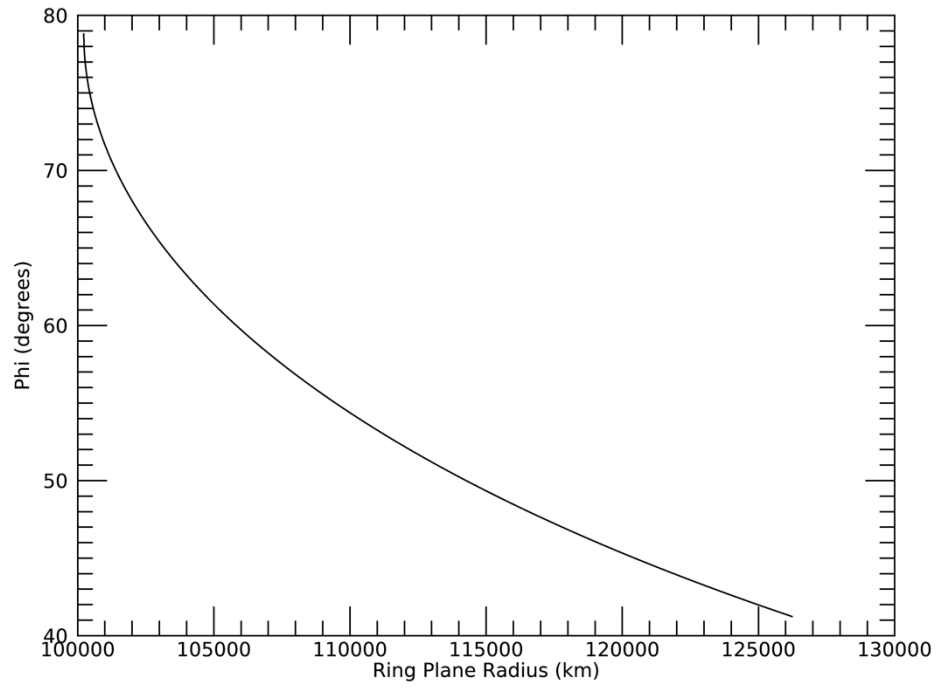
Rev 43I Signal

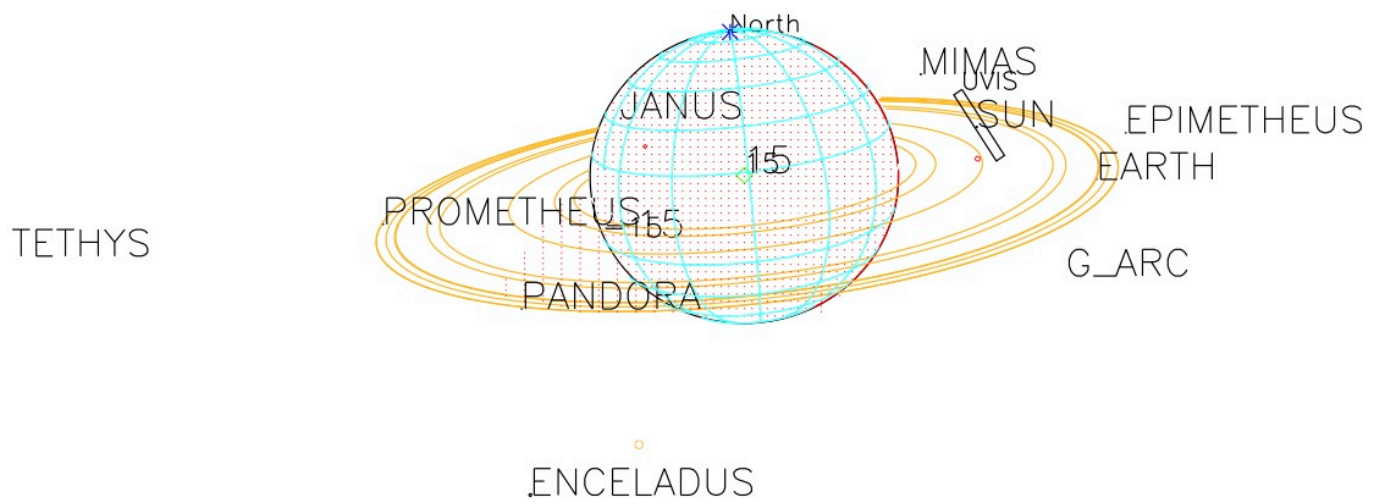


Rev 43I Radial Resolution



Rev 43I Phi





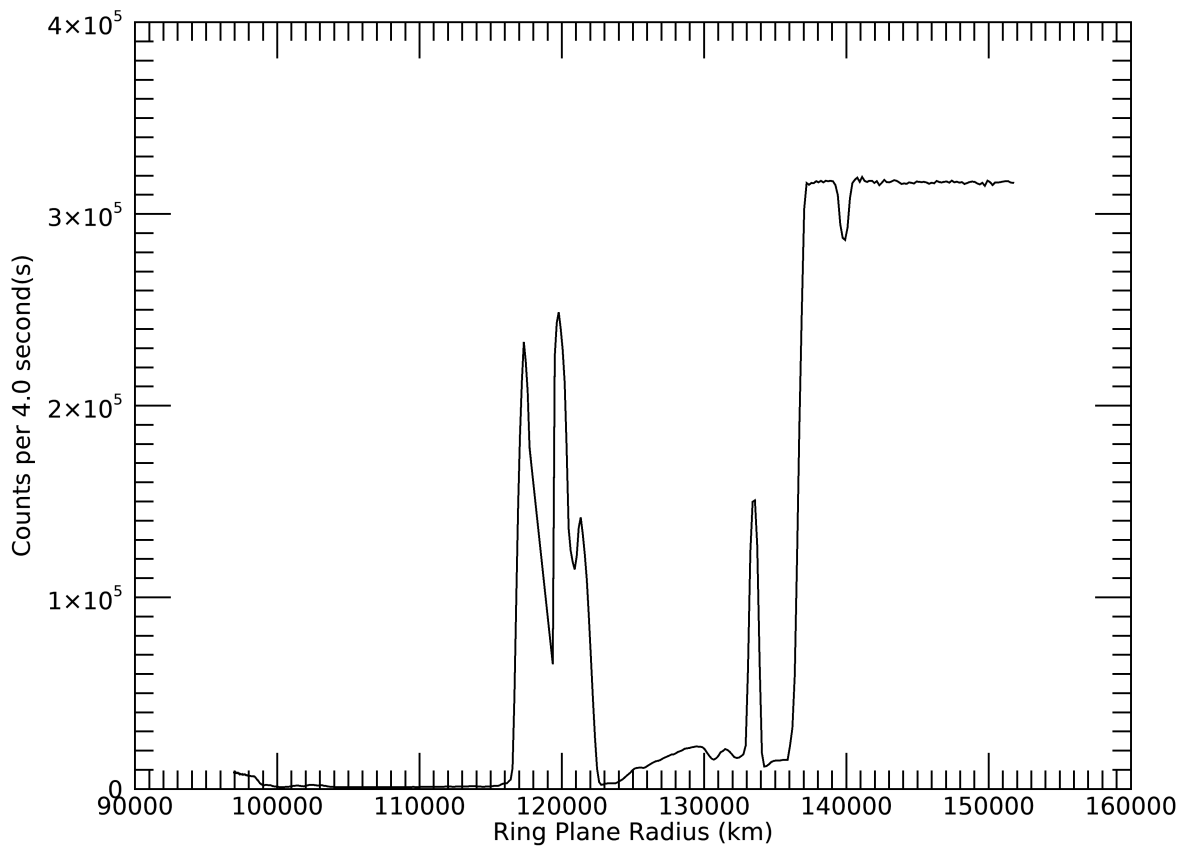
2007-114T10:17:00.000 457569.08 km

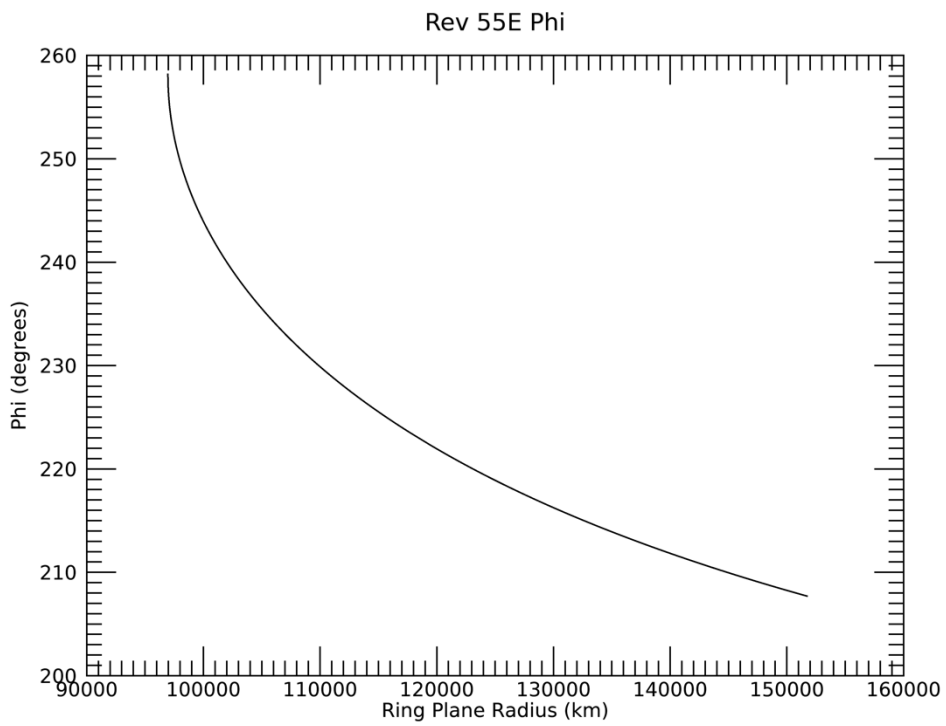
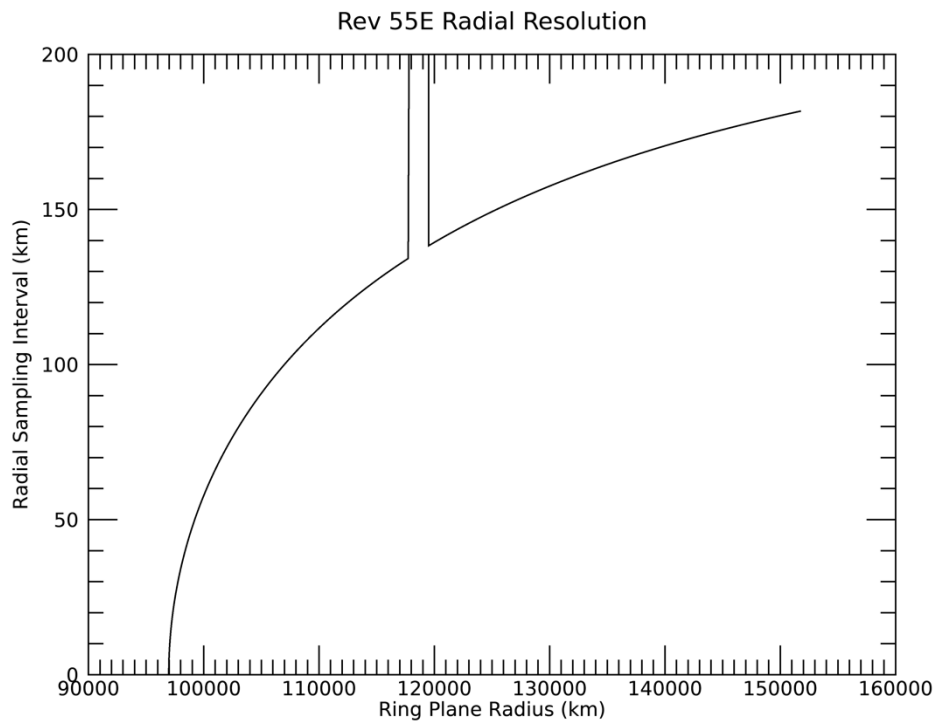
Target RA/dec: 338.59, -17.24

Subsolar lat/lon: -10.44, 76.60

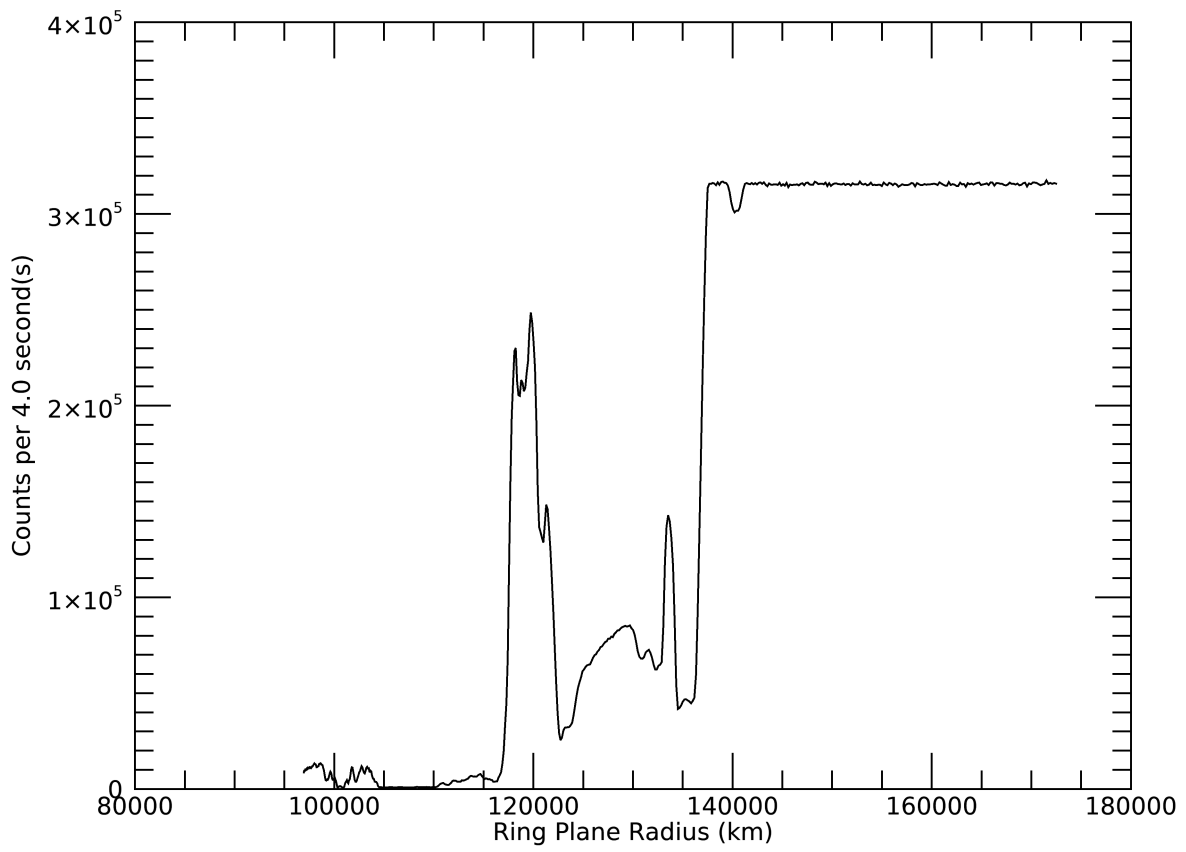
Sub-s/c lat/lon: 11.85, -91.62

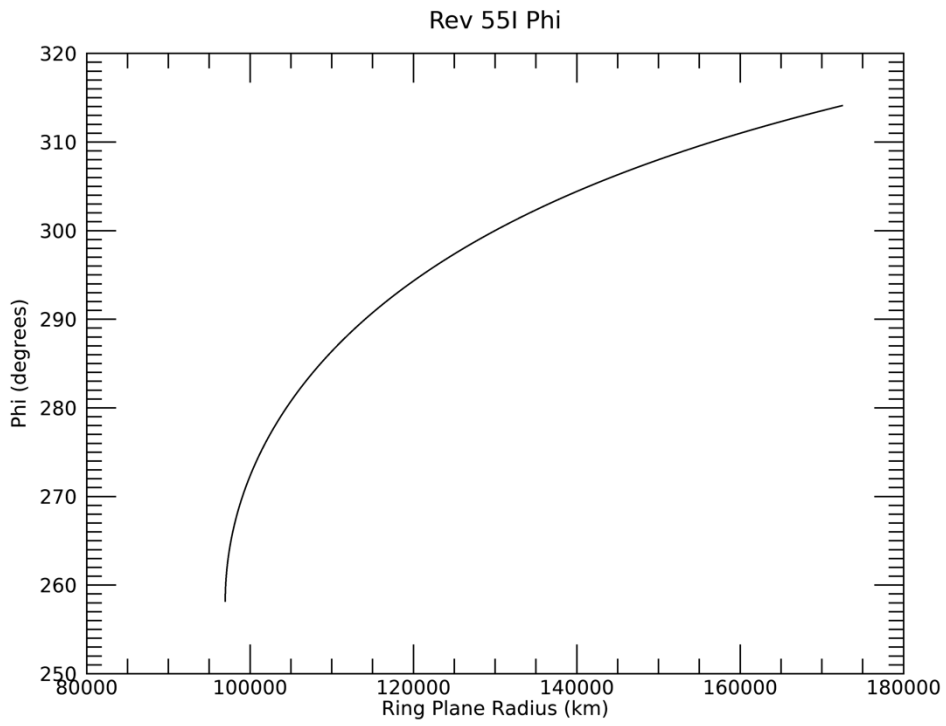
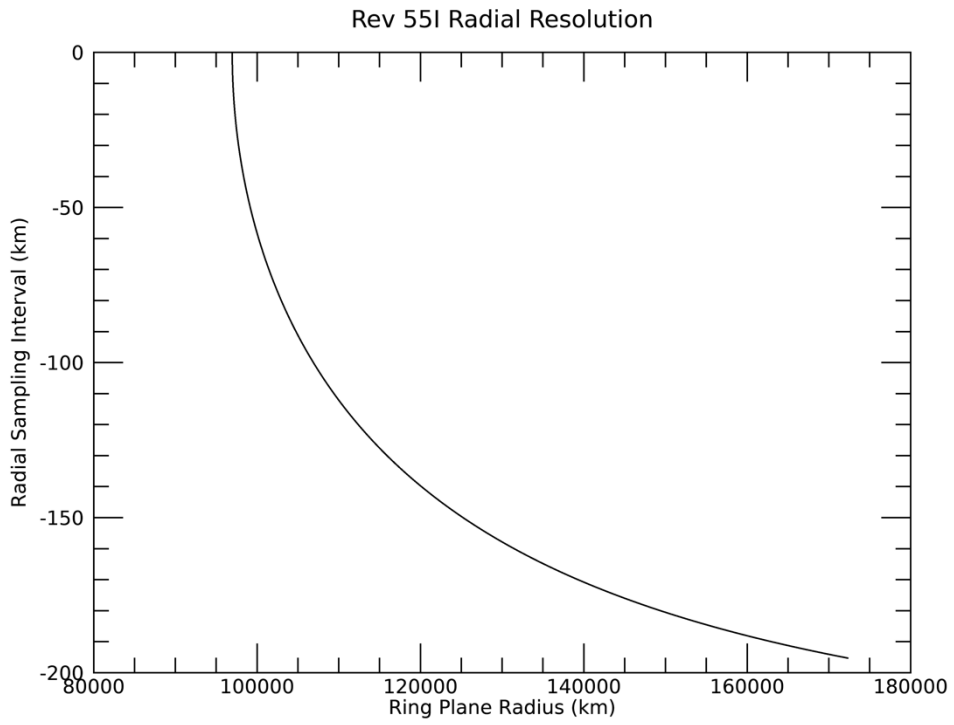
Rev 55E Signal

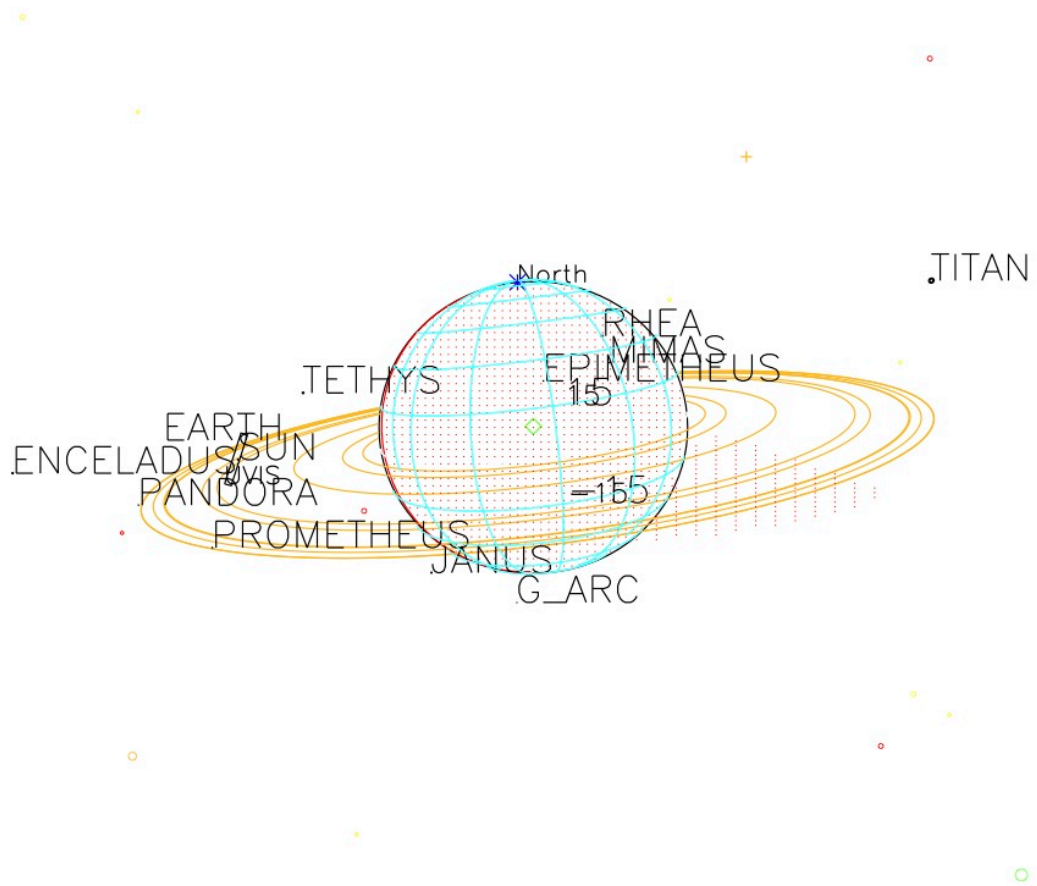




Rev 55I Signal







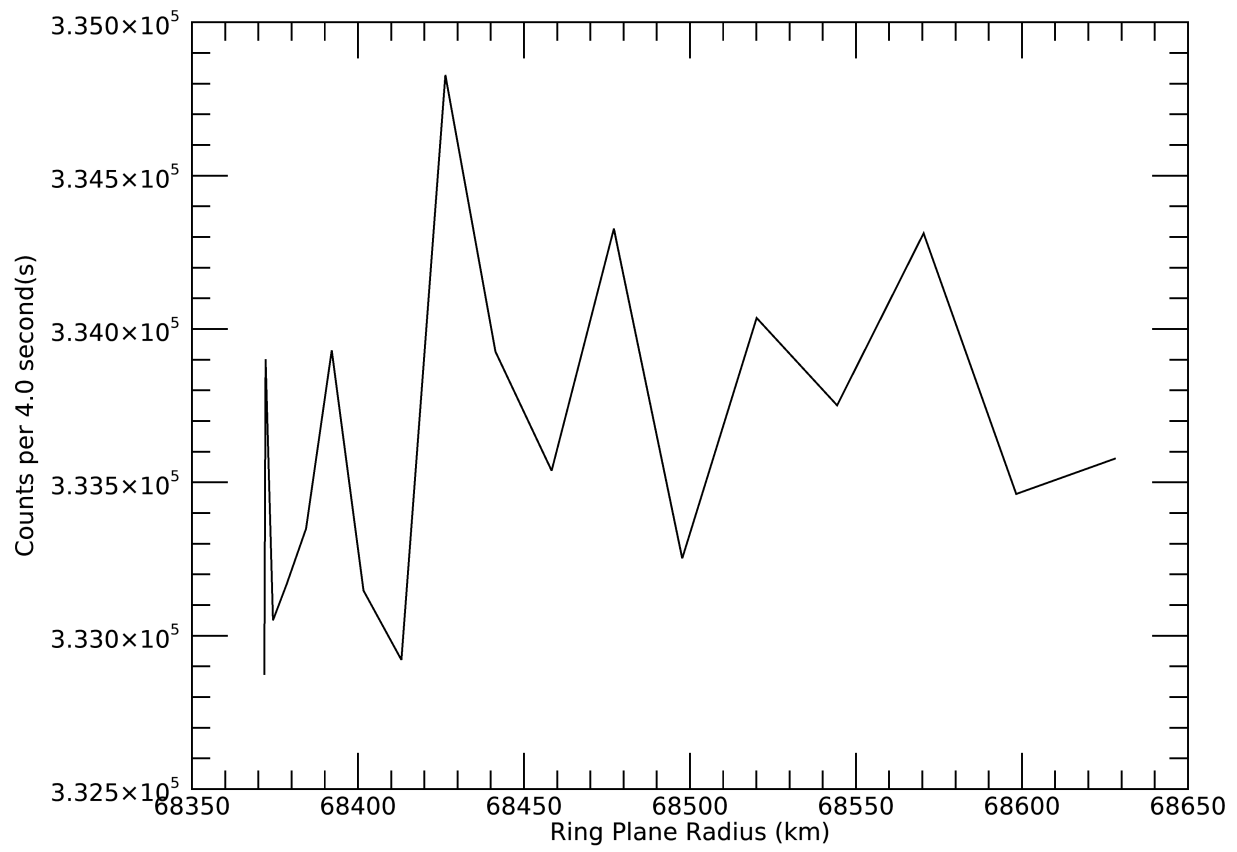
2008-003T20:36:00.000 291645.89 km

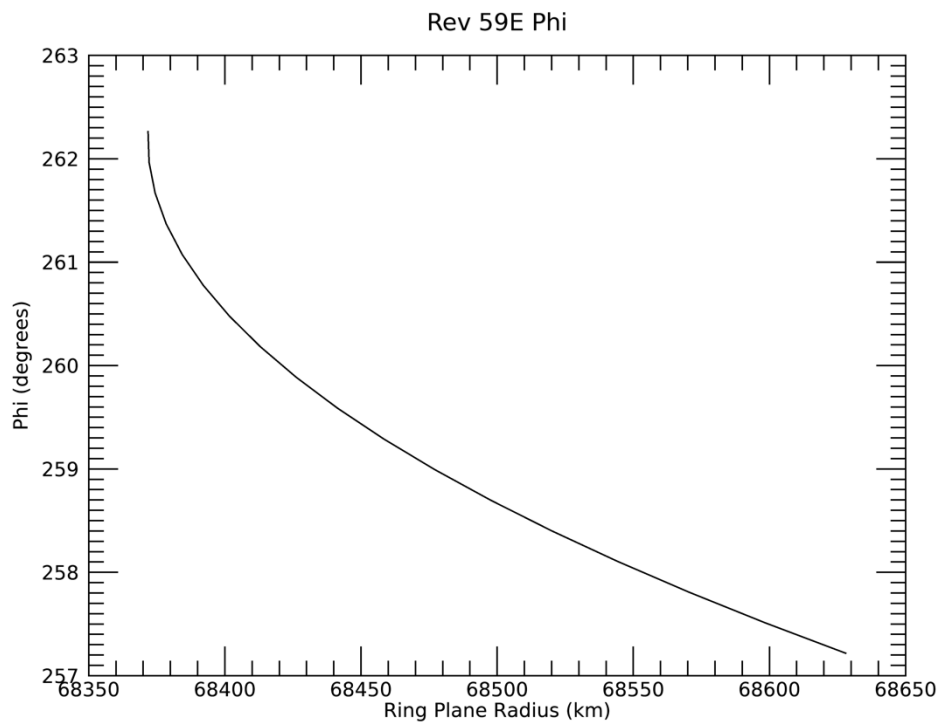
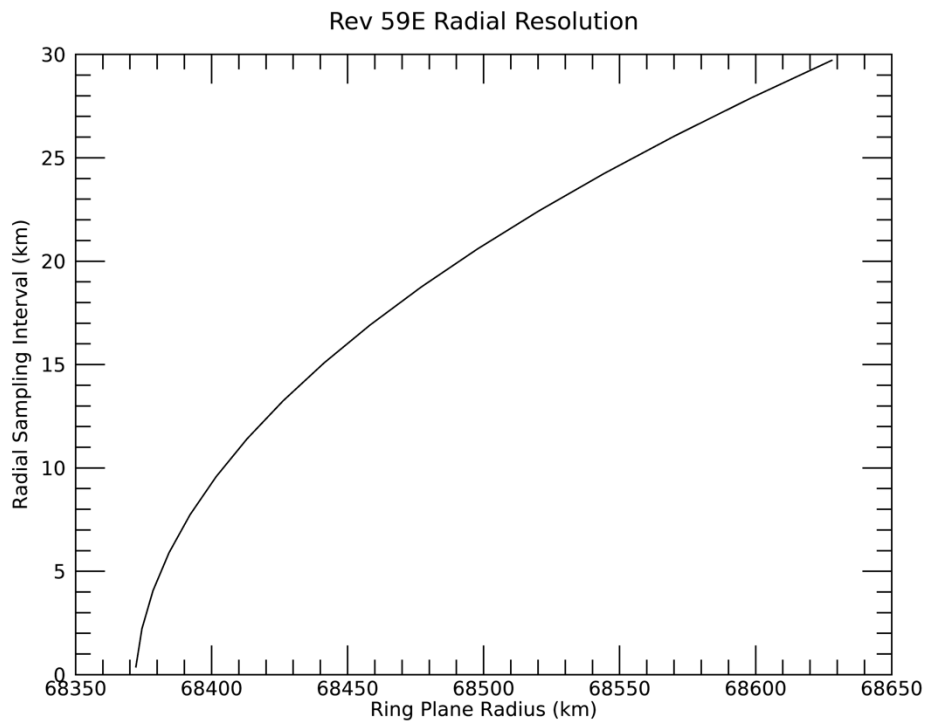
Target RA/dec: 313.26, -10.24

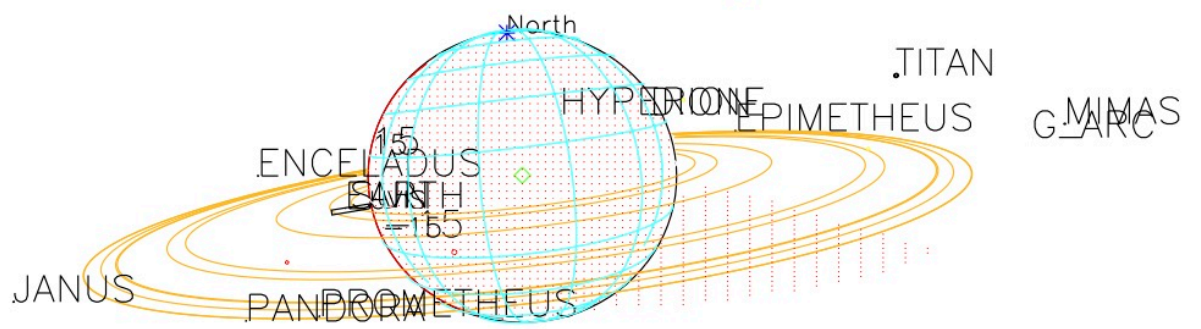
Subsolar lat/lon: -7.34, 74.82

Sub-s/c lat/lon: 8.38, -127.59

Rev 59E Signal







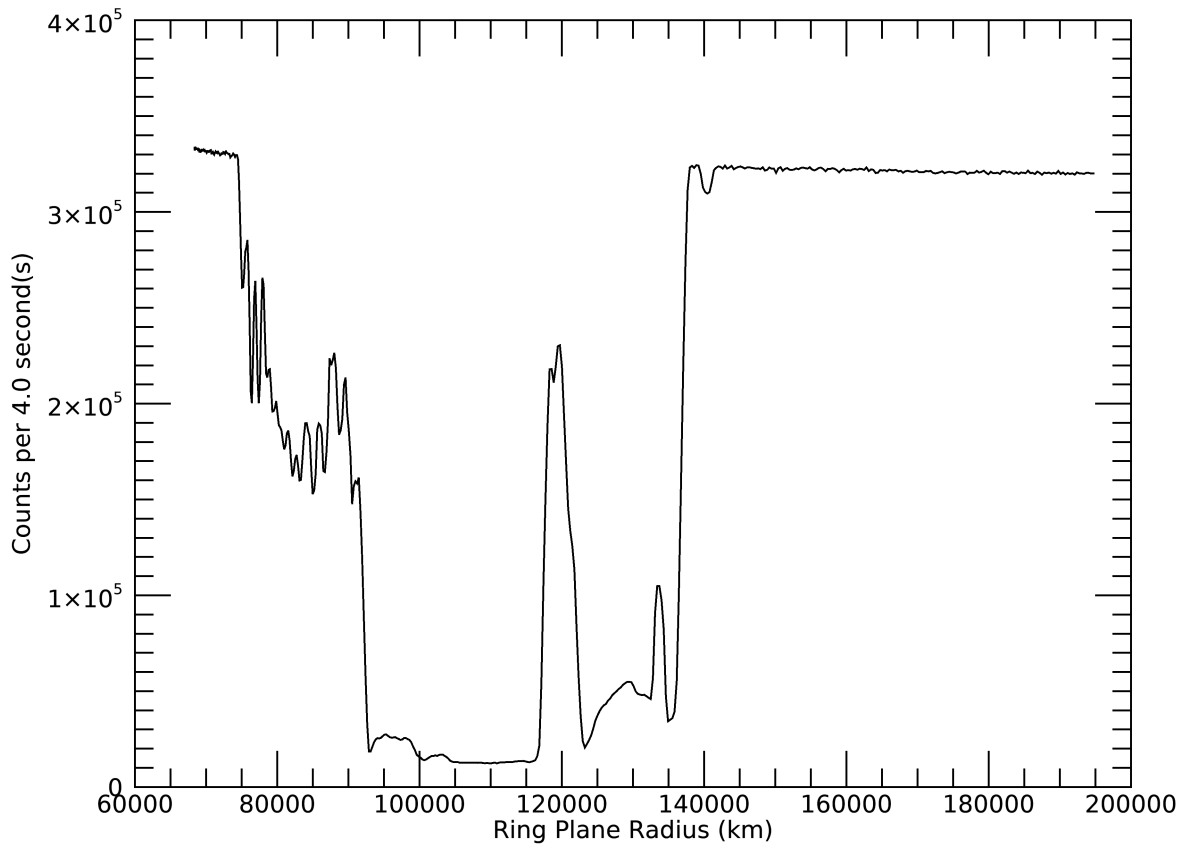
2008-051T17:14:00.000 218947.98 km

Target RA/dec: 319.34, -8.49

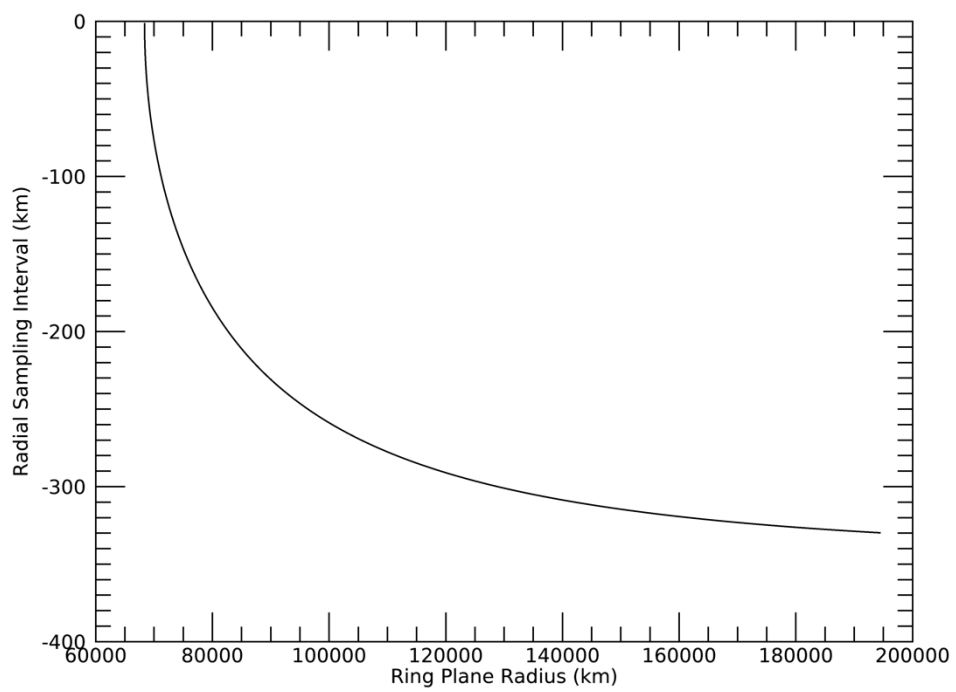
Subsolar lat/lon: -6.75, 151.99

Sub-s/c lat/lon: 6.40, -46.12

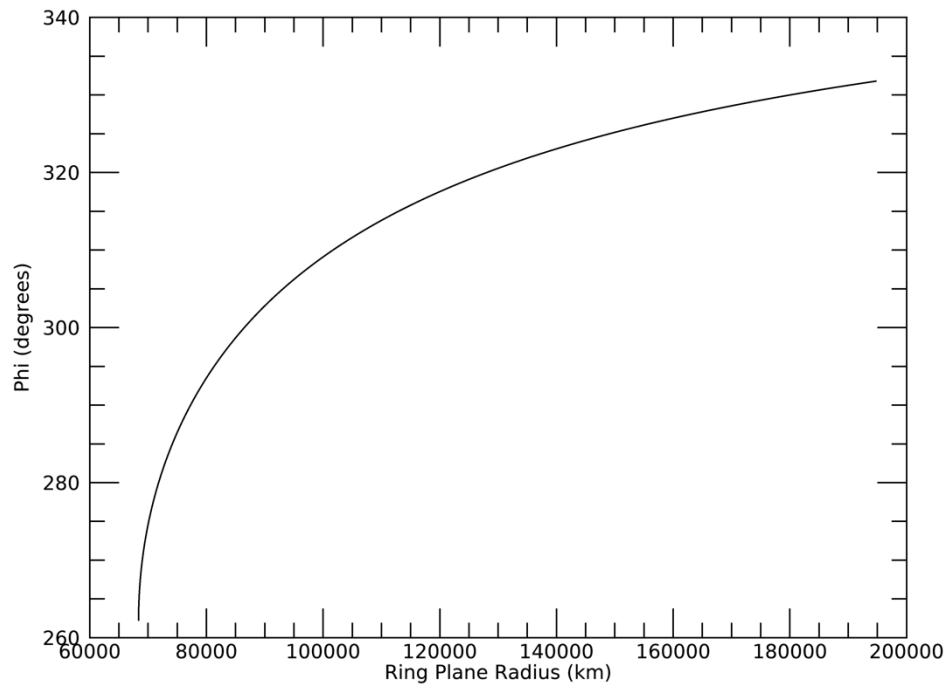
Rev 59I Signal

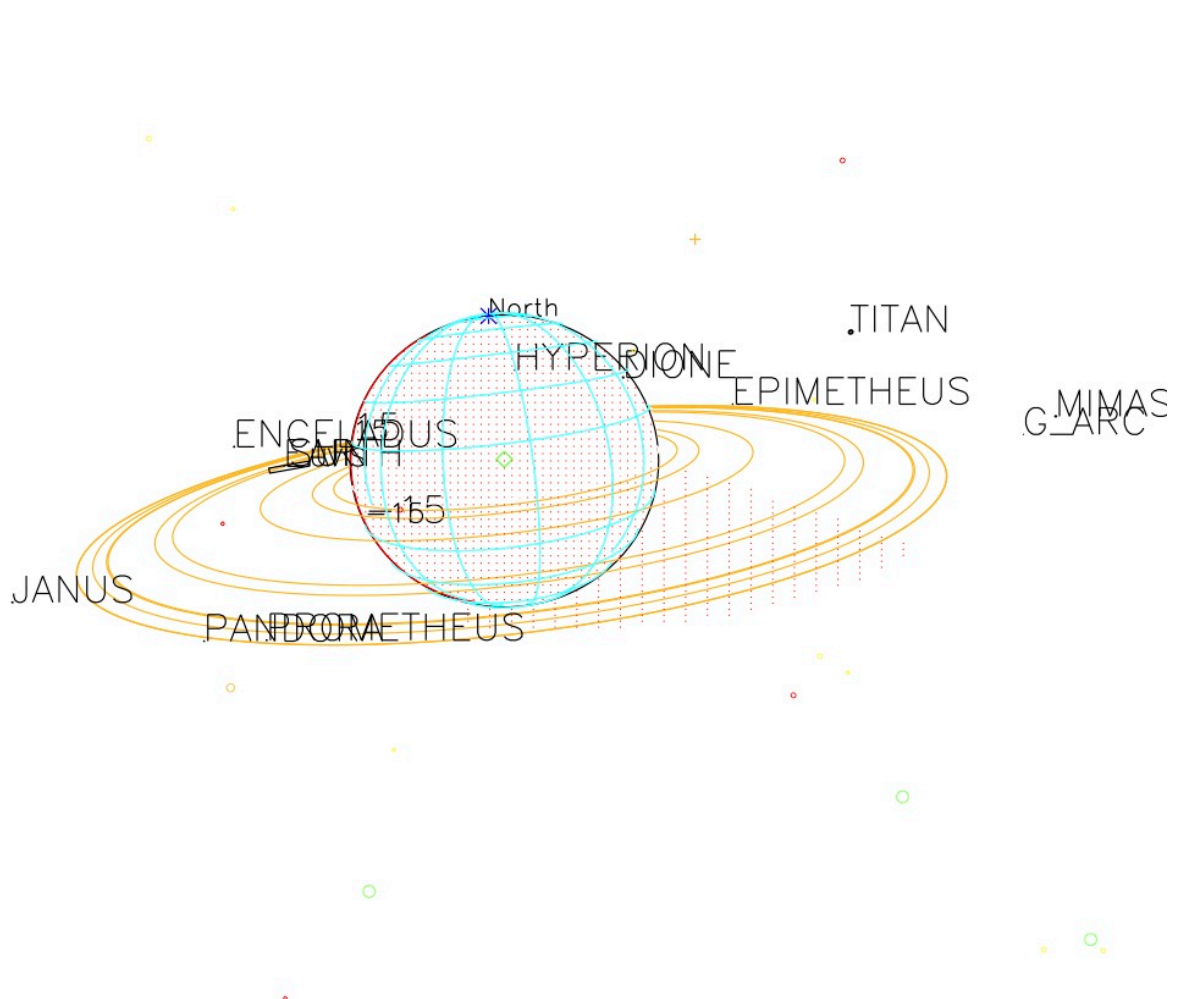


Rev 59I Radial Resolution



Rev 59I Phi





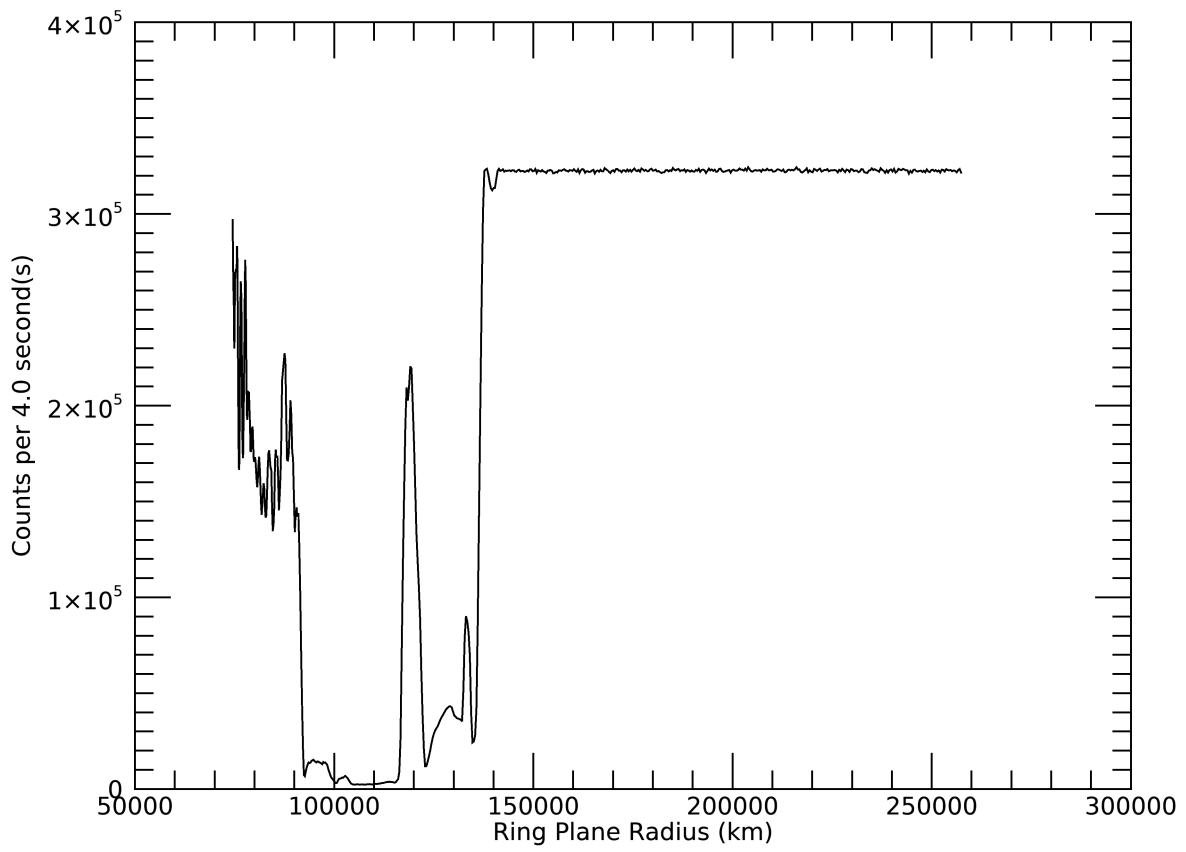
2008-051T16:56:00.000 224869.15 km

Target RA/dec: 315.74, -11.45

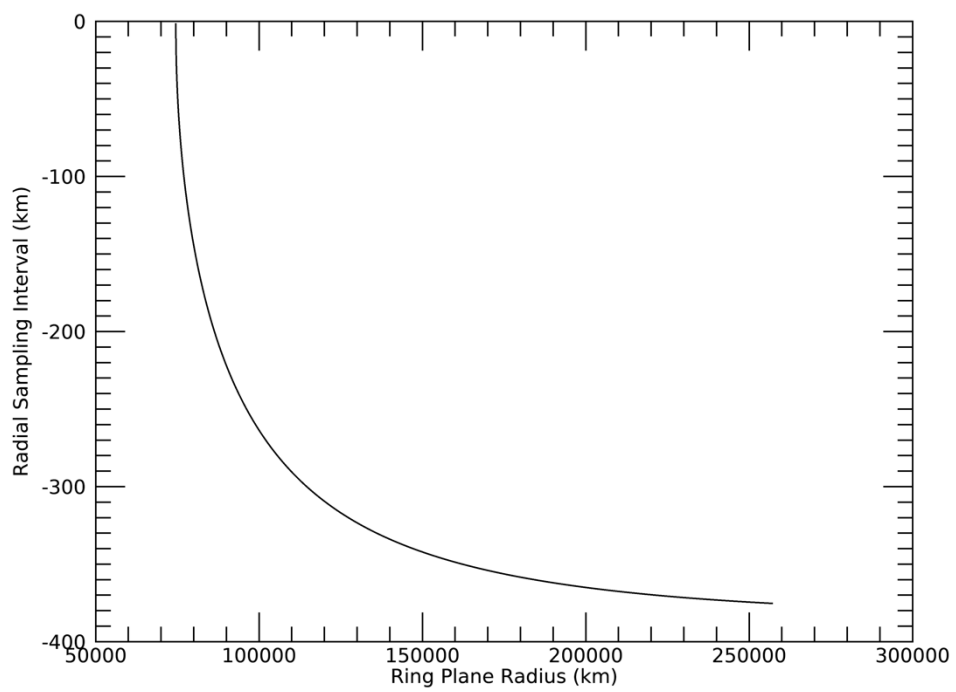
Subsolar lat/lon: -6.75, 162.13

Sub-s/c lat/lon: 9.27, -39.22

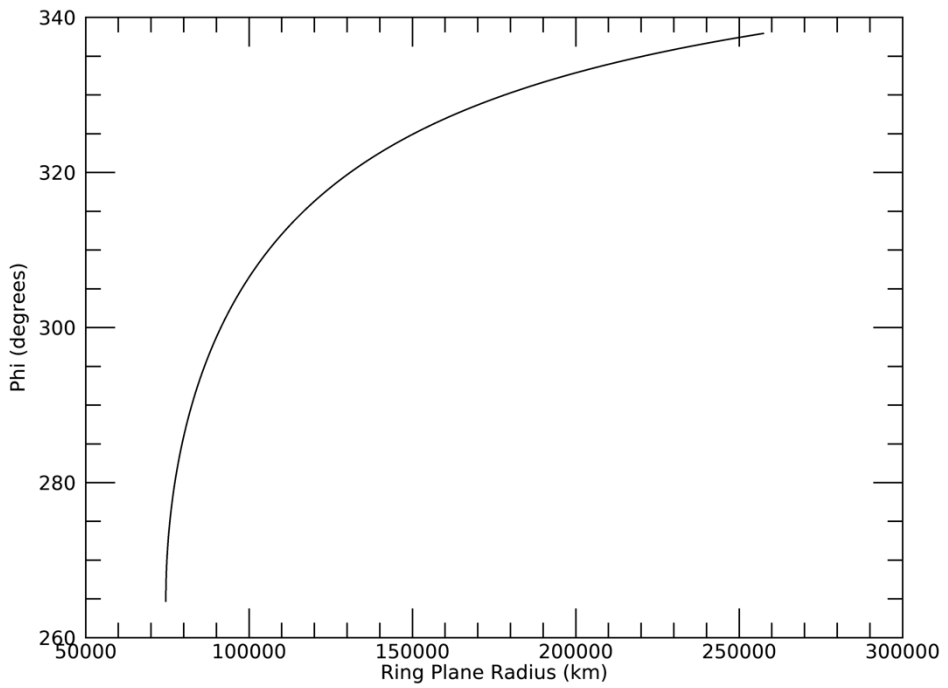
Rev 62I Signal

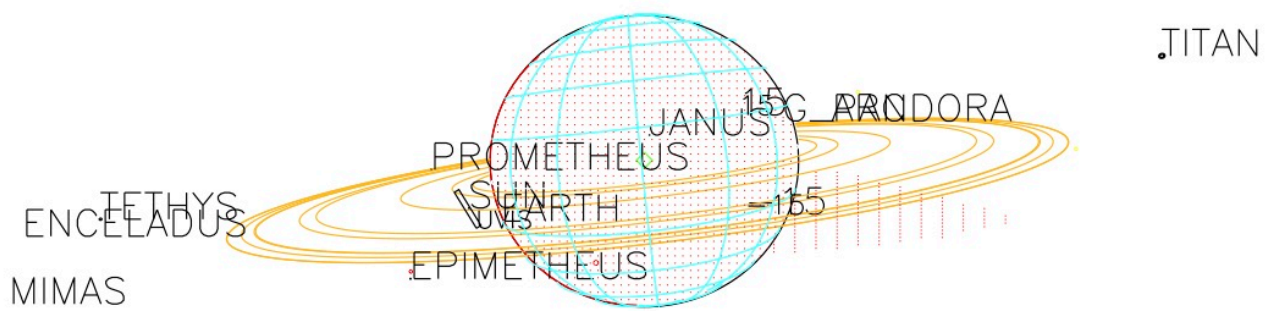


Rev 62I Radial Resolution



Rev 62I Phi





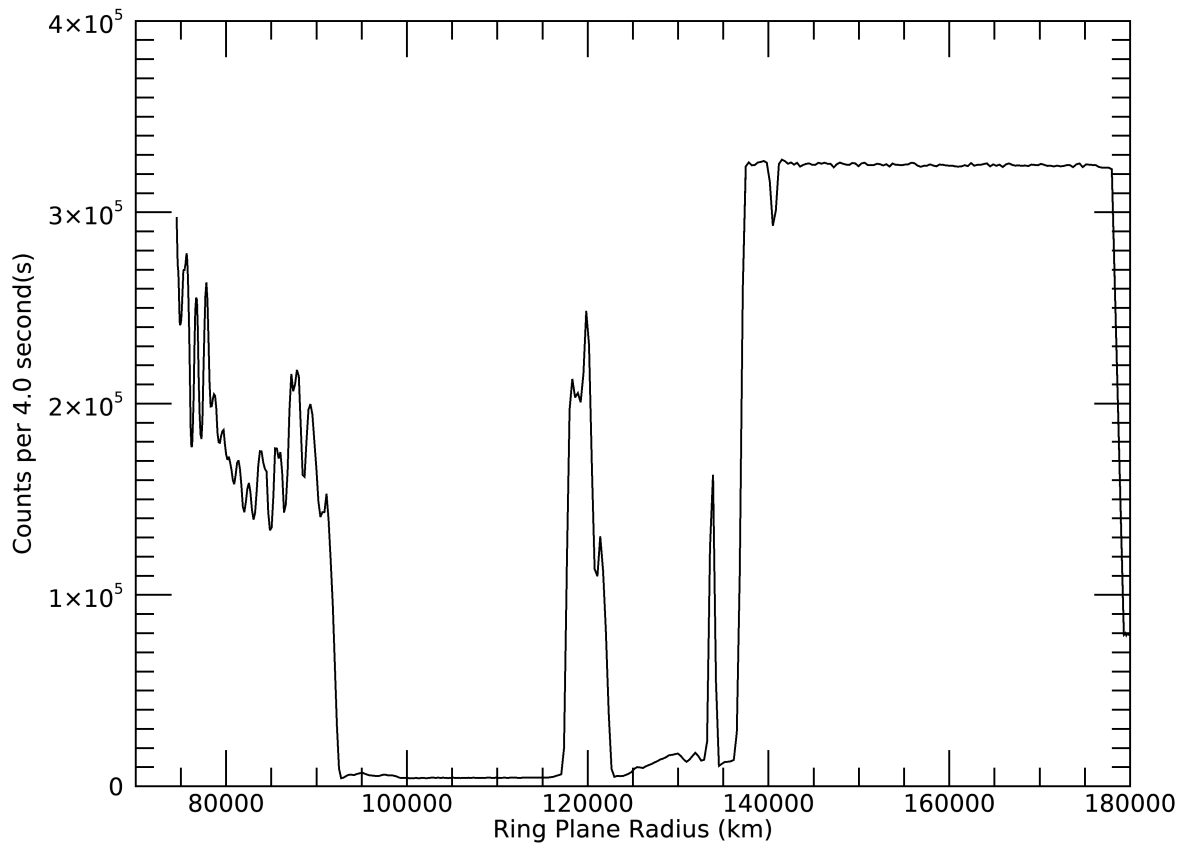
2008-083T09:50:00.000 244924.94 km

Target RA/dec: 322.08, -7.01

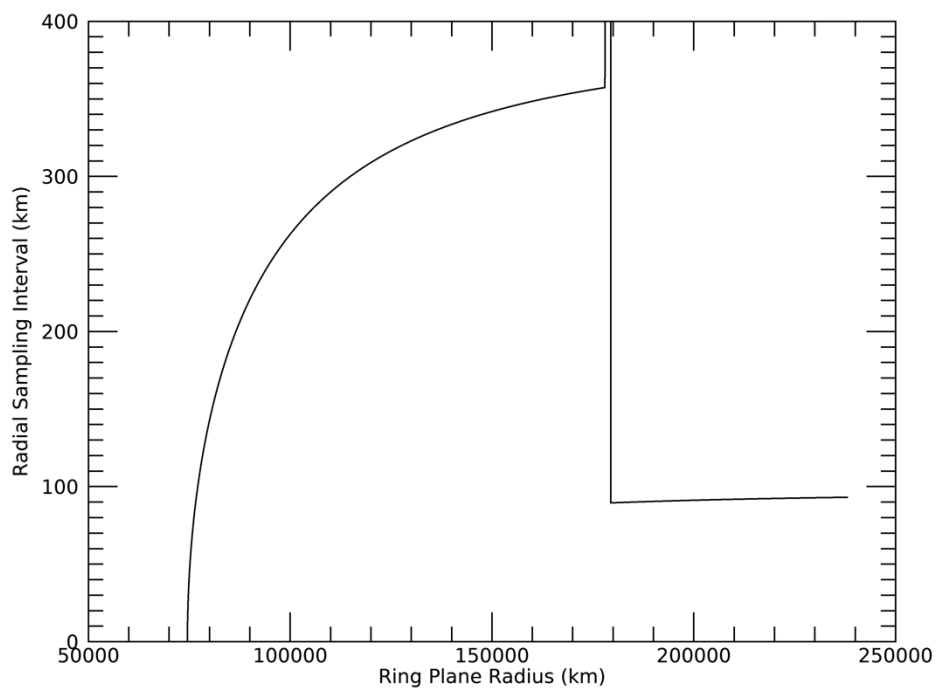
Subsolar lat/lon: -6.35, 17.60

Sub-s/c lat/lon: 4.85, -178.98

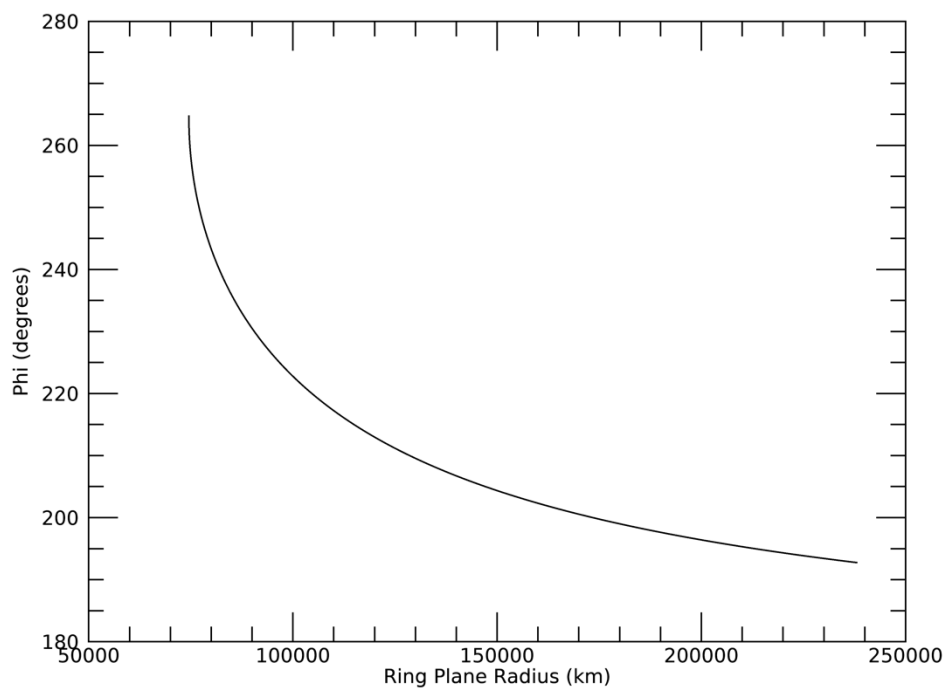
Rev 62E Signal

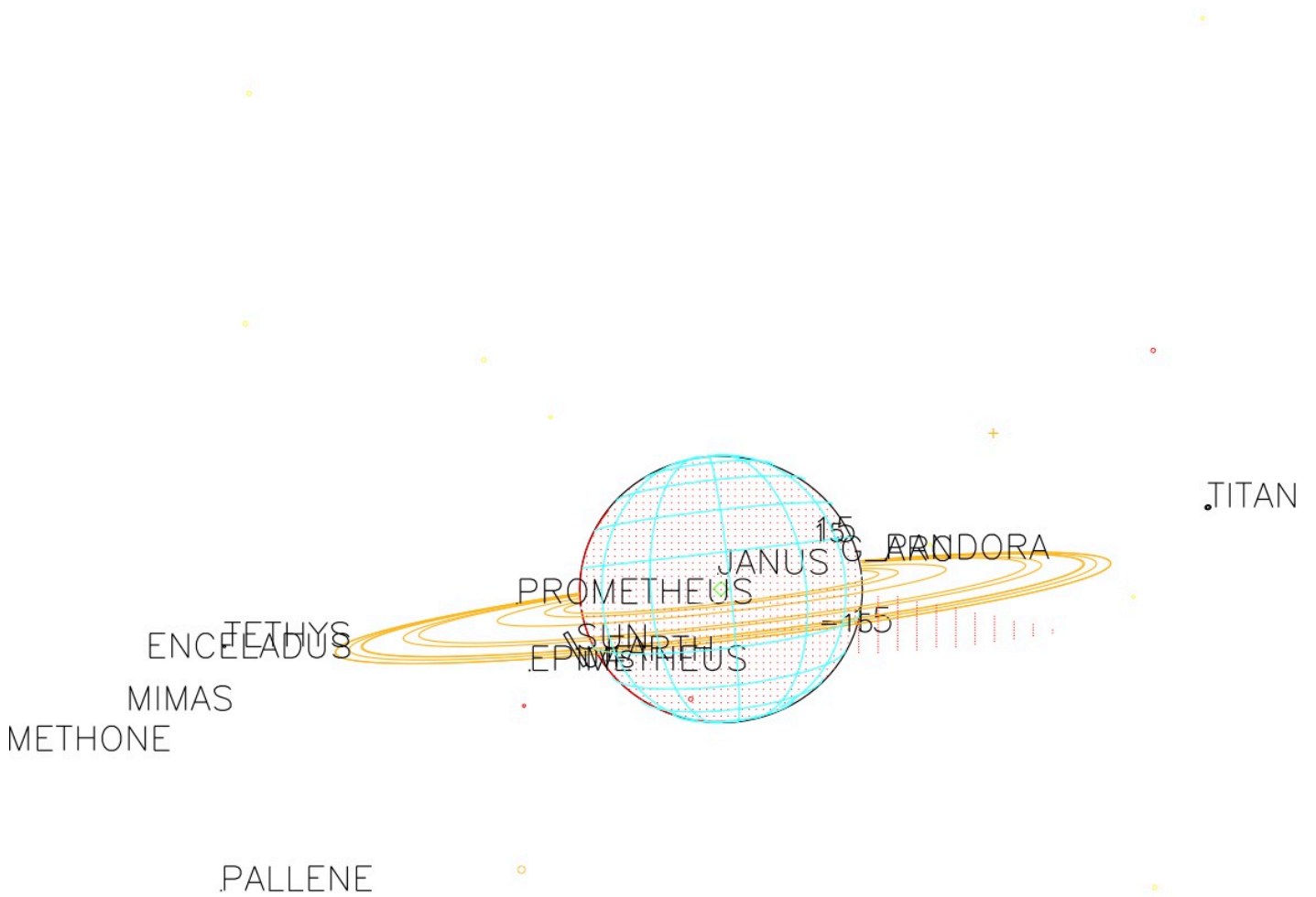


Rev 62E Radial Resolution



Rev 62E Phi





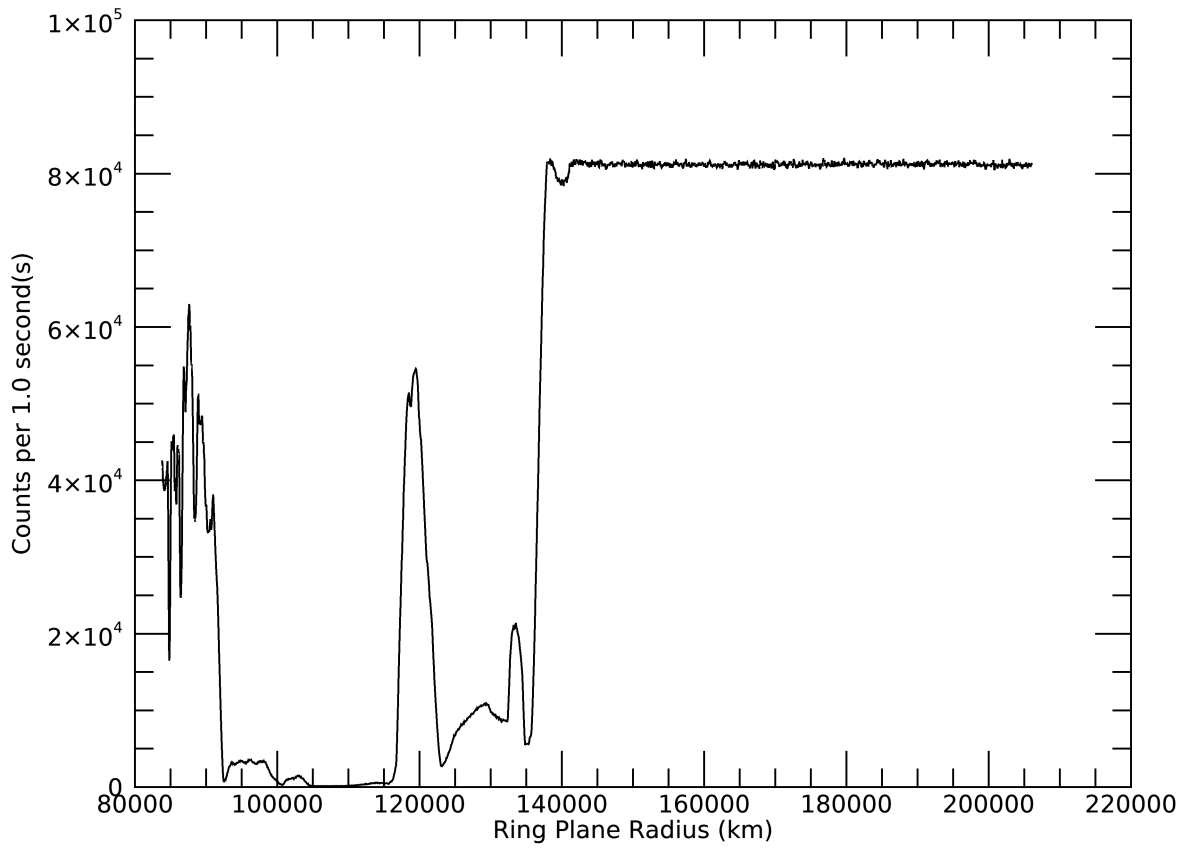
2008-083T10:00:00.000 242464.43 km

Target RA/dec: 323.55, -5.30

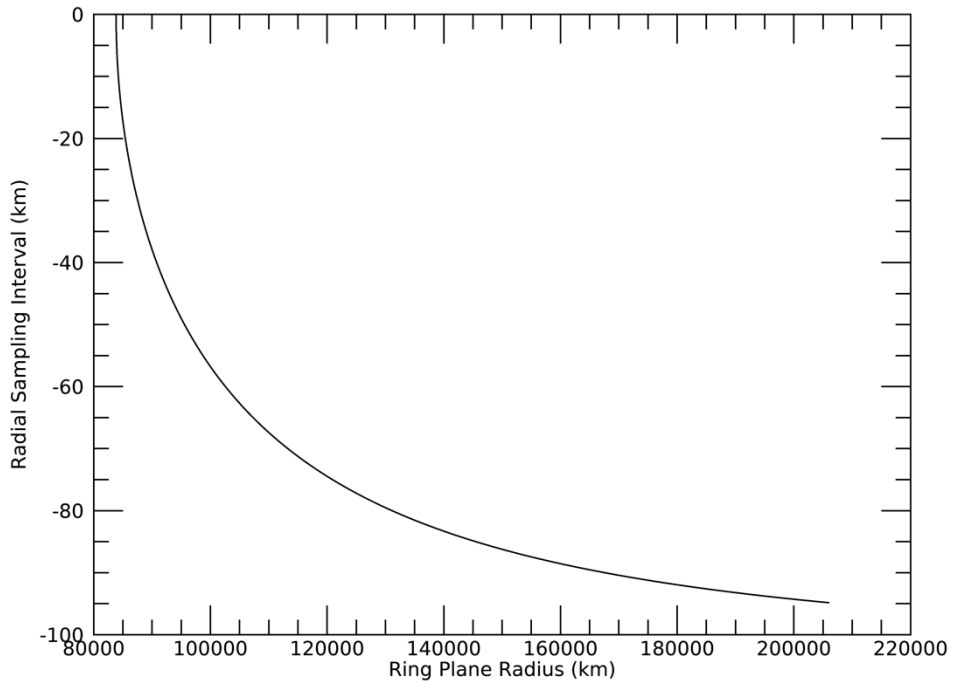
Subsolar lat/lon: -6.35, 11.97

Sub-s/c lat/lon: 3.26, 176.65

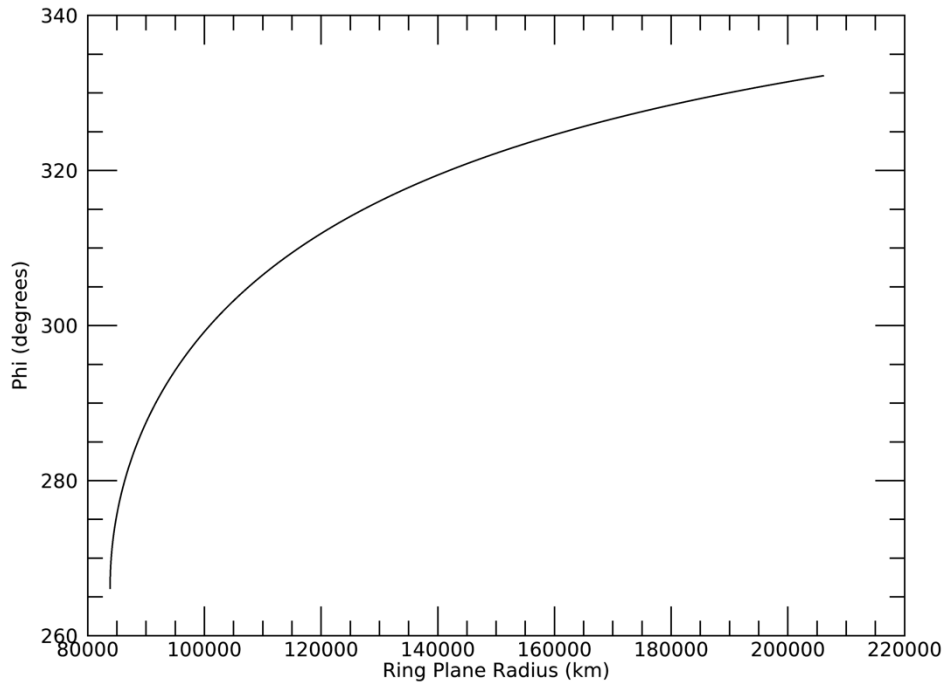
Rev 65I Signal

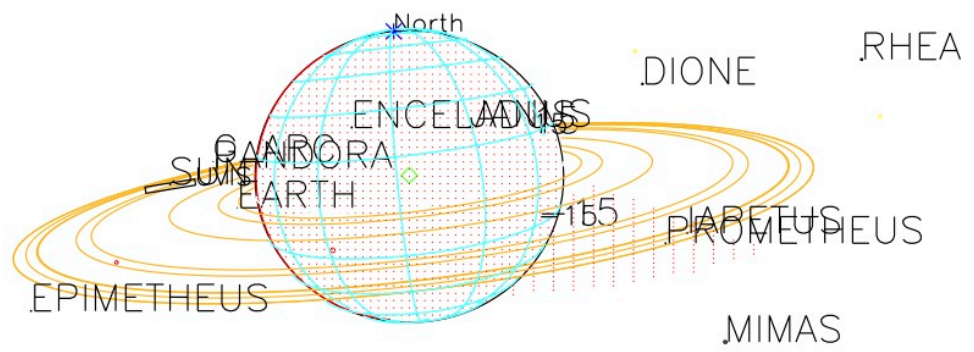


Rev 65I Radial Resolution



Rev 65I Phi





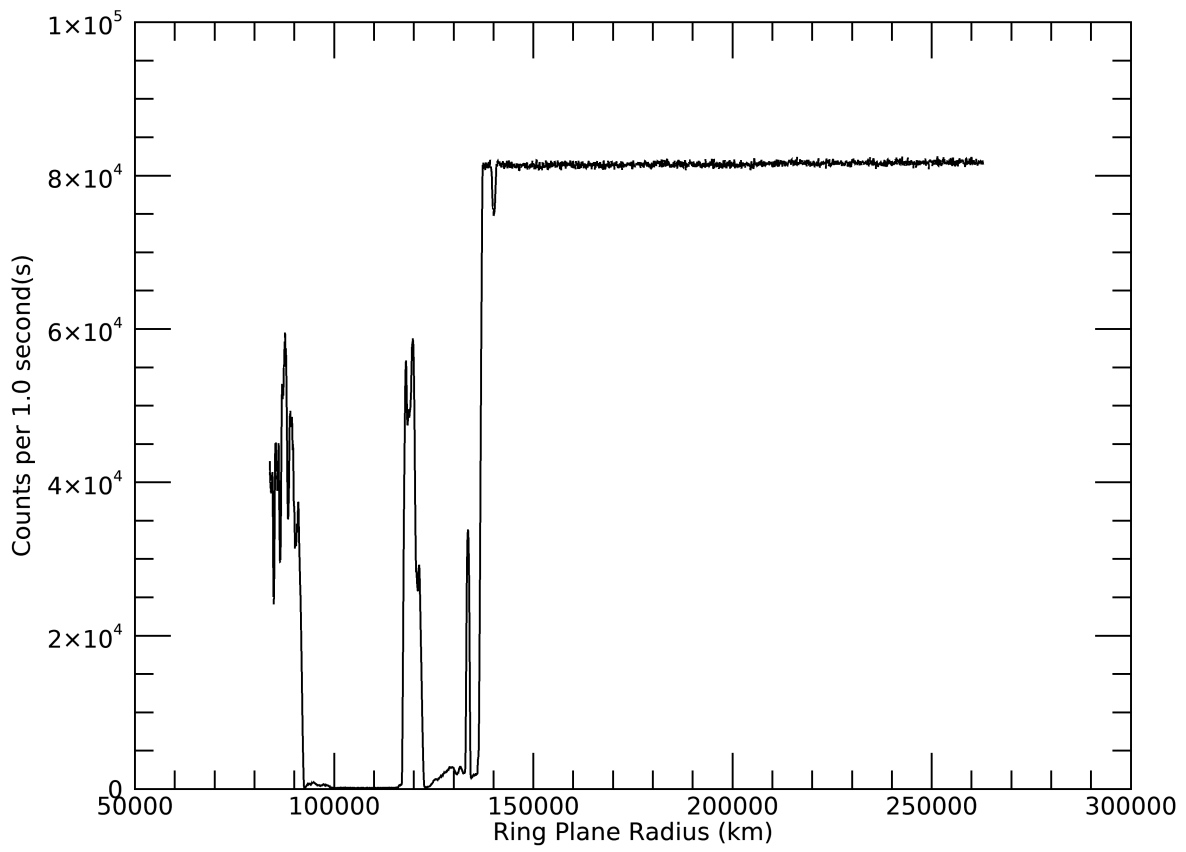
2008-111T20:35:00.000 282077.20 km

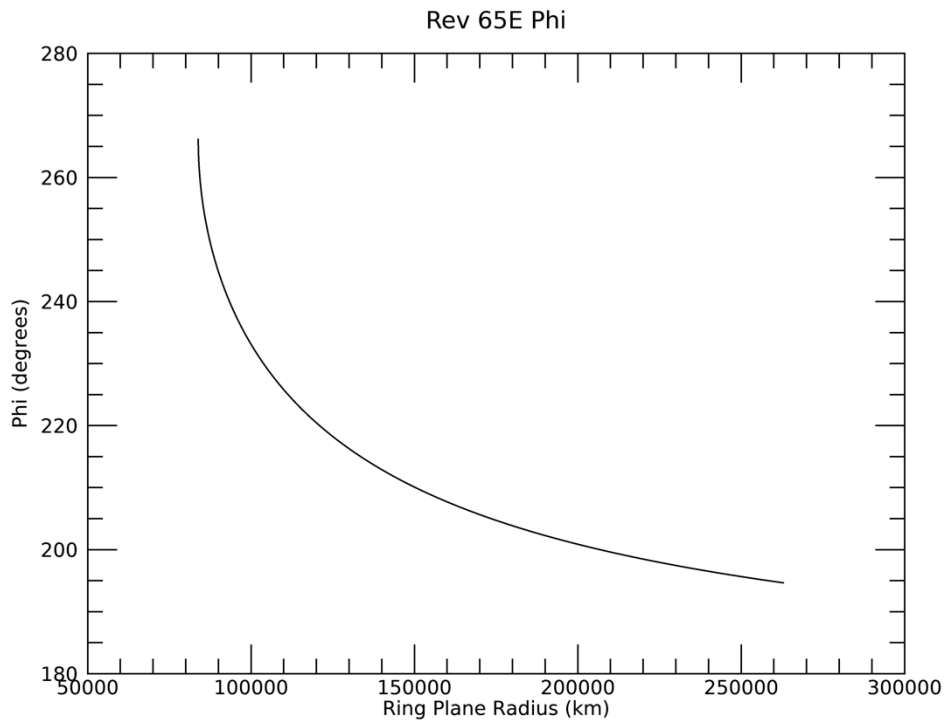
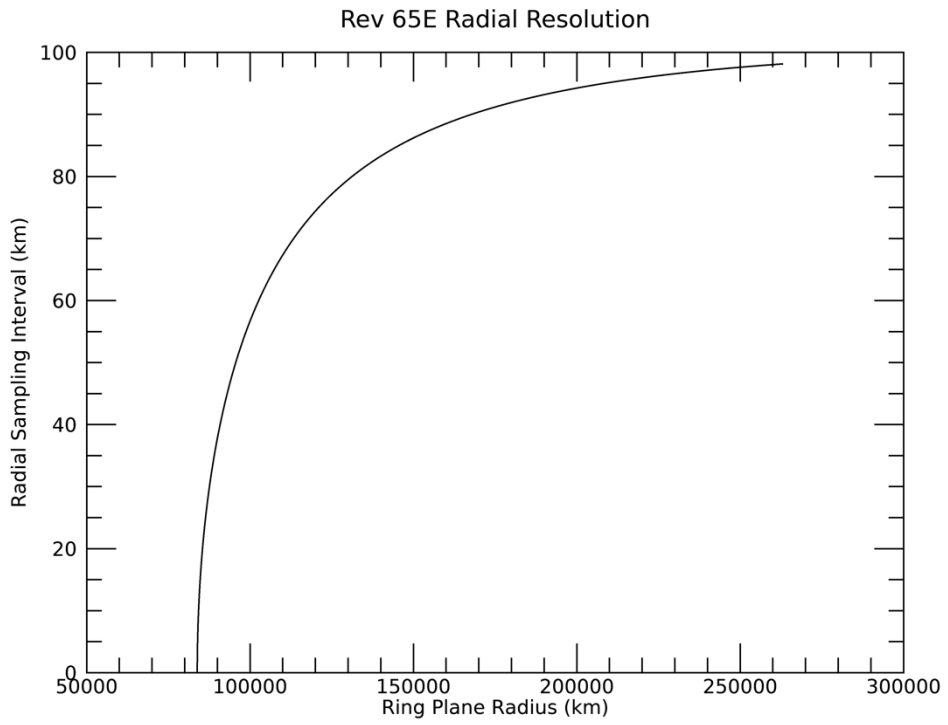
Target RA/dec: 320.34, -10.42

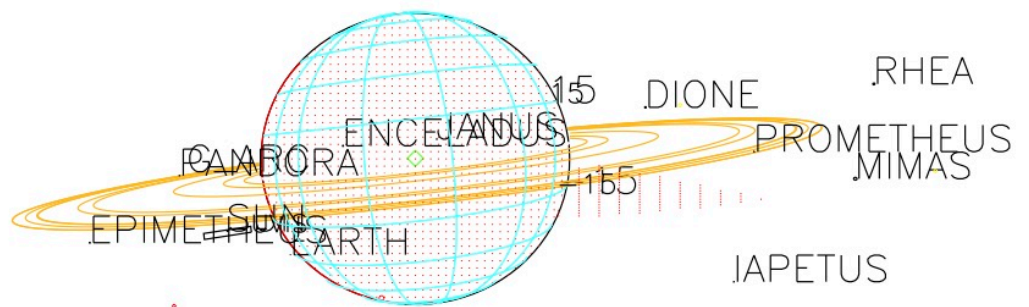
Subsolar lat/lon: -6.00, -6.88

Sub-s/c lat/lon: 7.87, 154.27

Rev 65E Signal







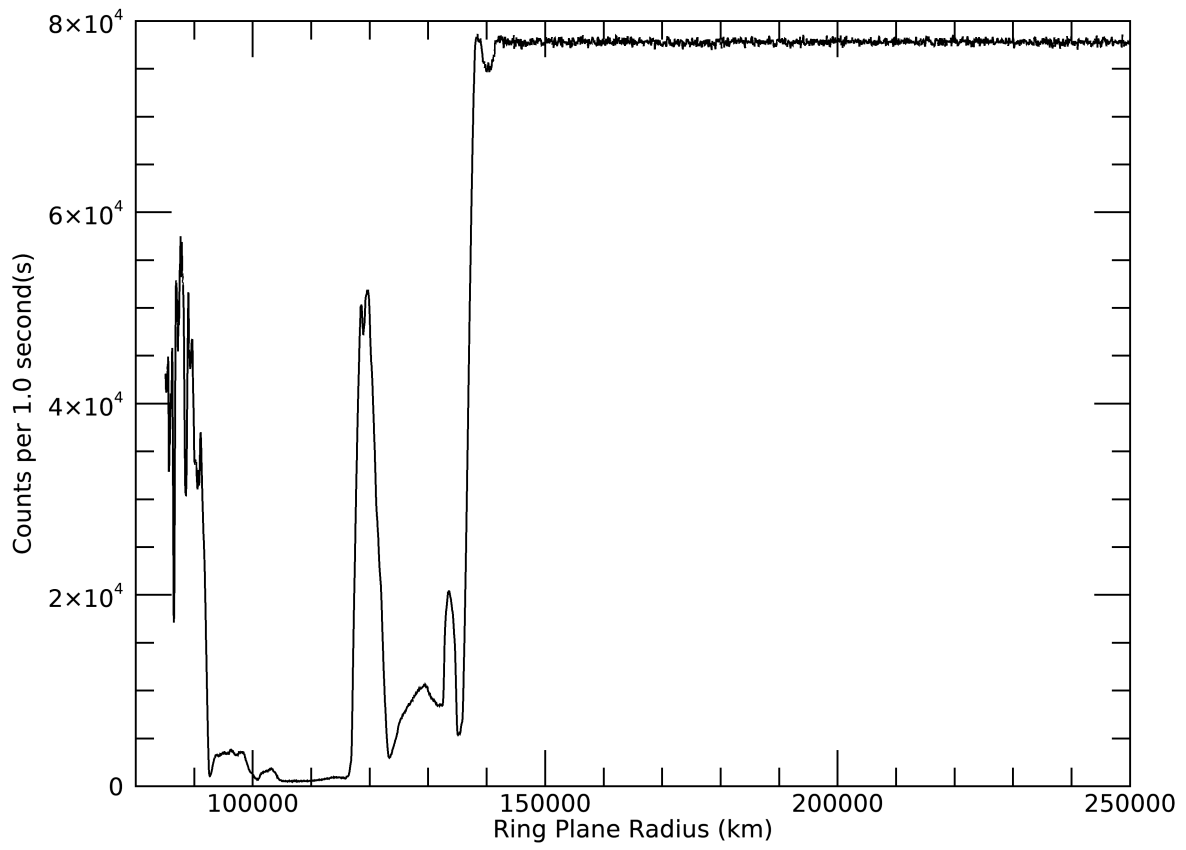
2008-111T21:10:00.000 274618.51 km

Target RA/dec: 323.88, -5.11

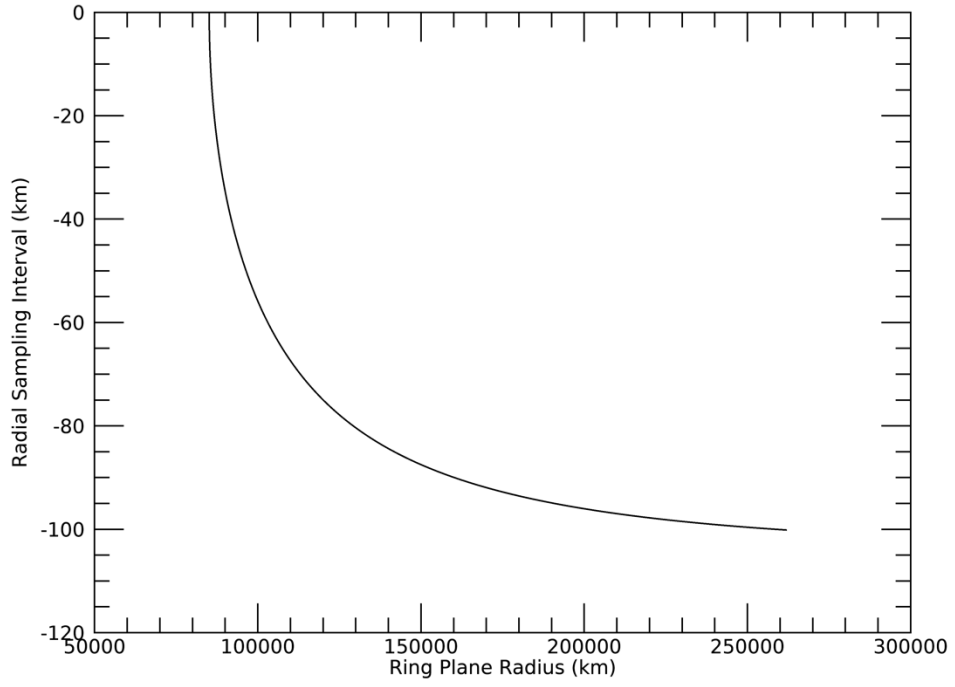
Subsolar lat/lon: -6.00, -26.59

Sub-s/c lat/lon: 3.05, 137.49

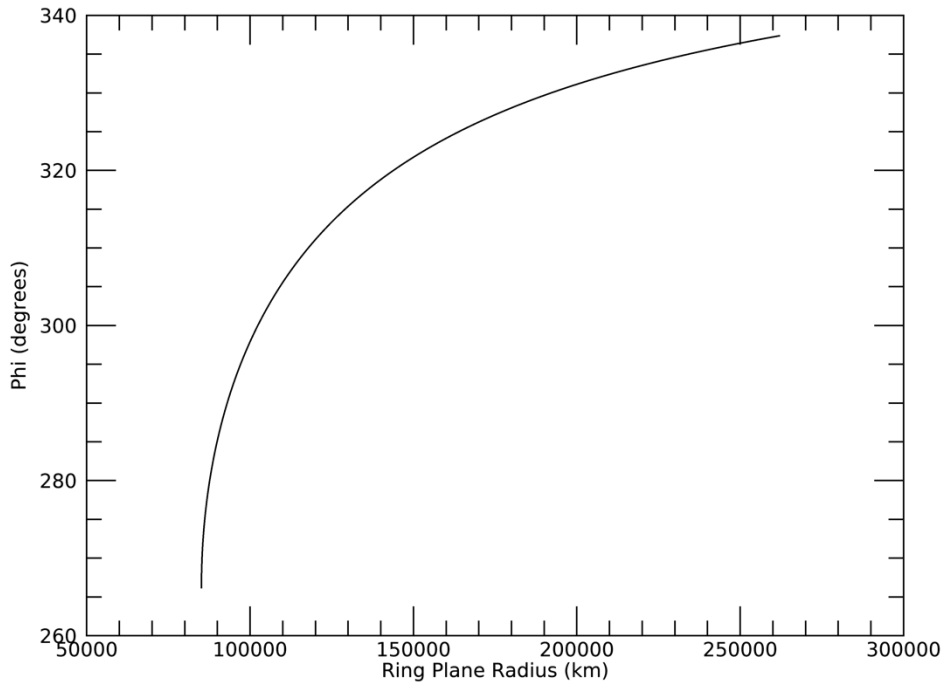
Rev 66I Signal

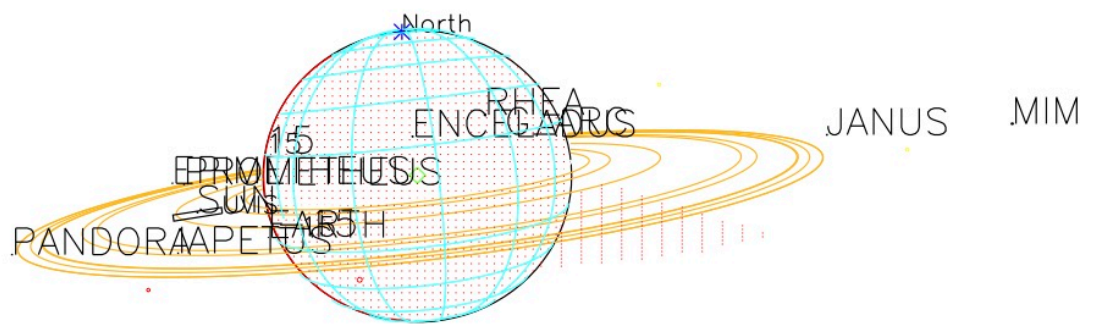


Rev 66I Radial Resolution



Rev 66I Phi





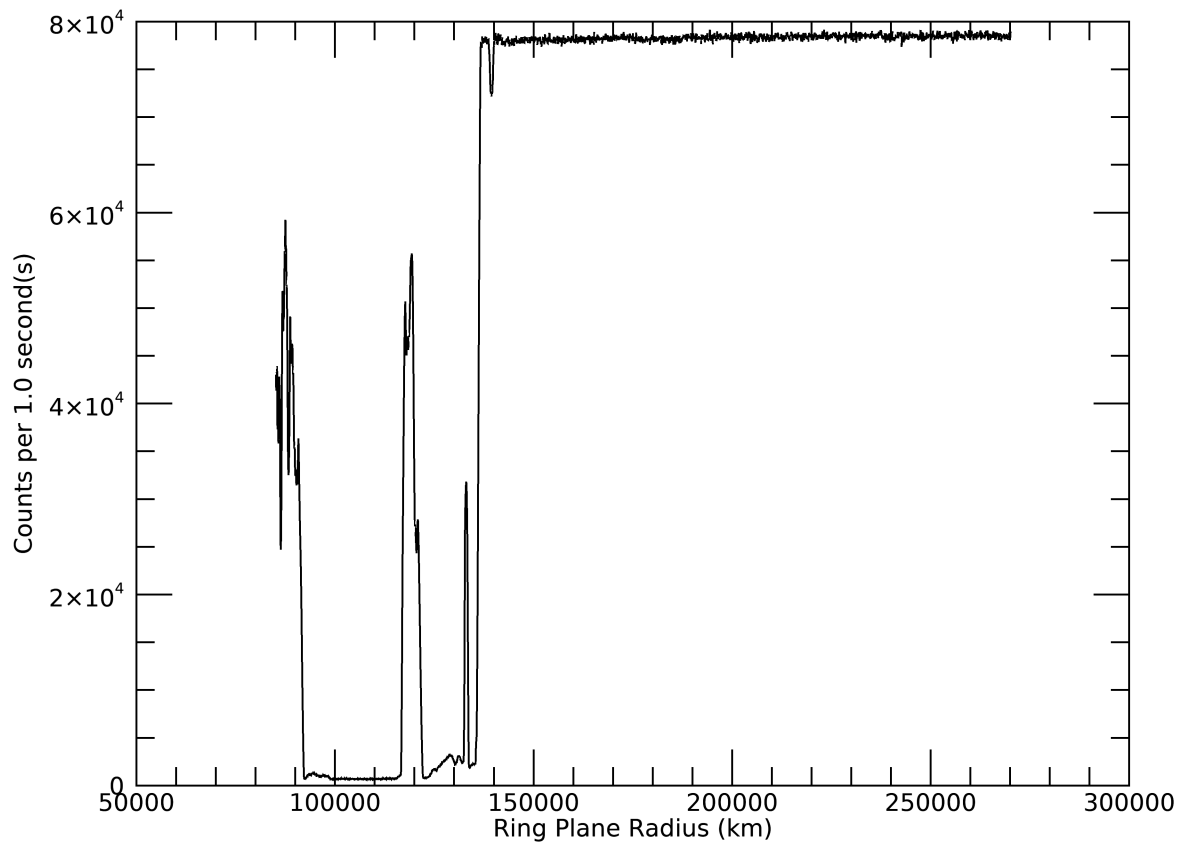
2008-121T10:04:00.000 277993.81 km

Target RA/dec: 321.87, -7.99

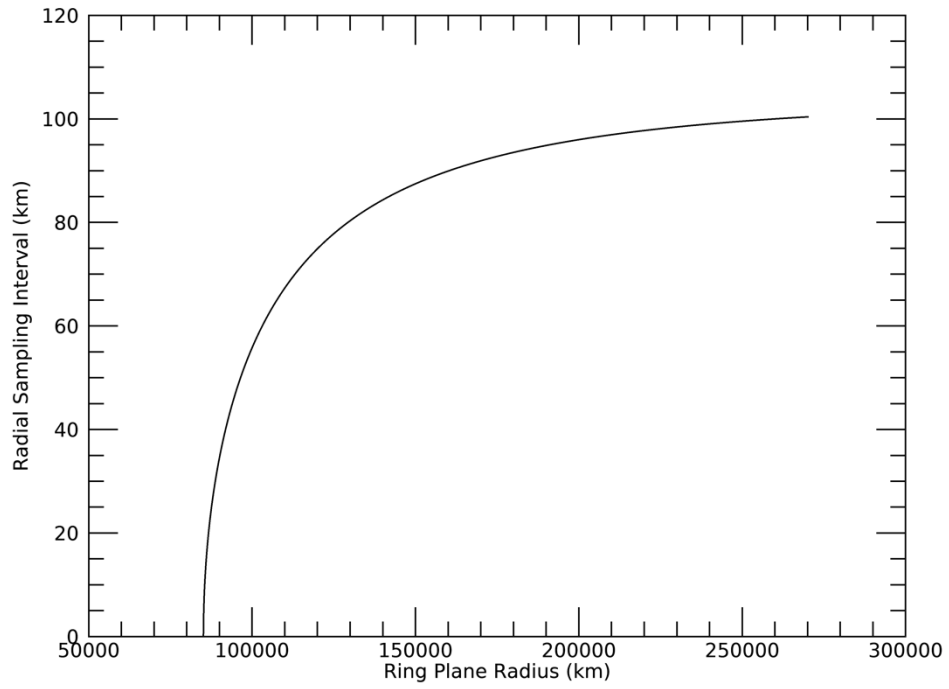
Subsolar lat/lon: -5.88, 160.77

Sub-s/c lat/lon: 5.67, -37.13

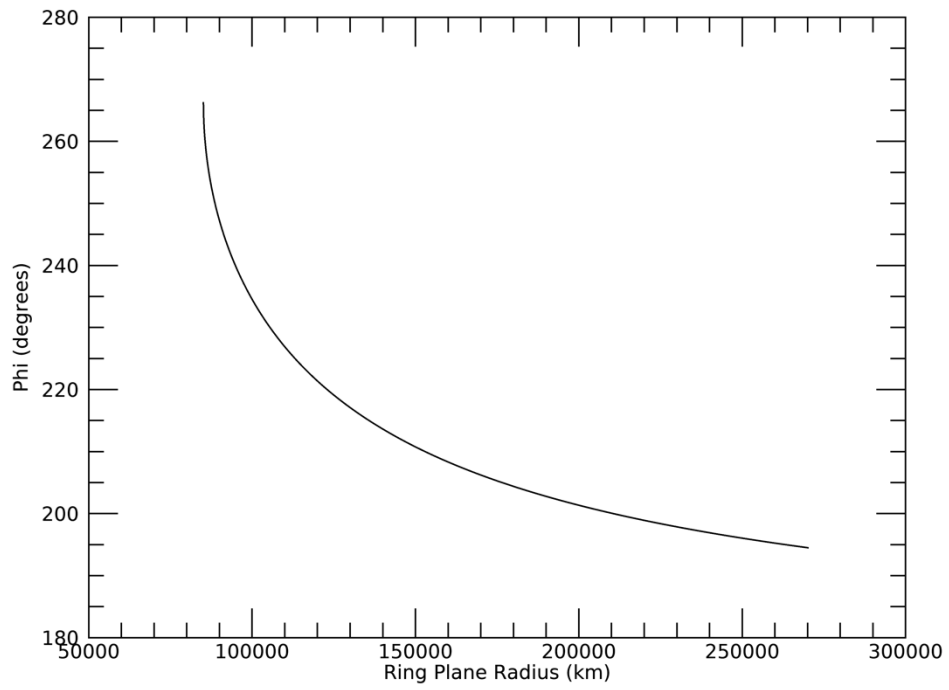
Rev 66E Signal

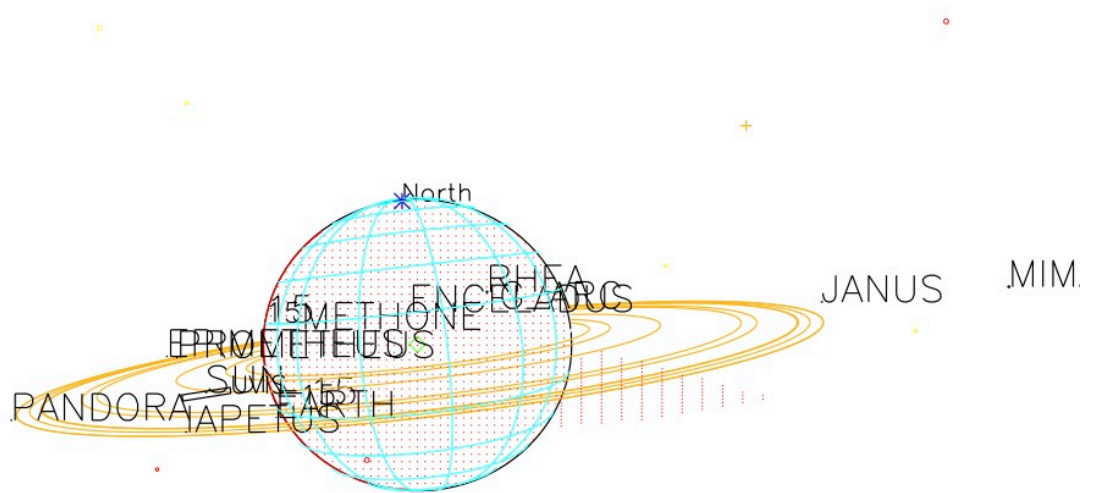


Rev 66E Radial Resolution



Rev 66E Phi





PALLENE

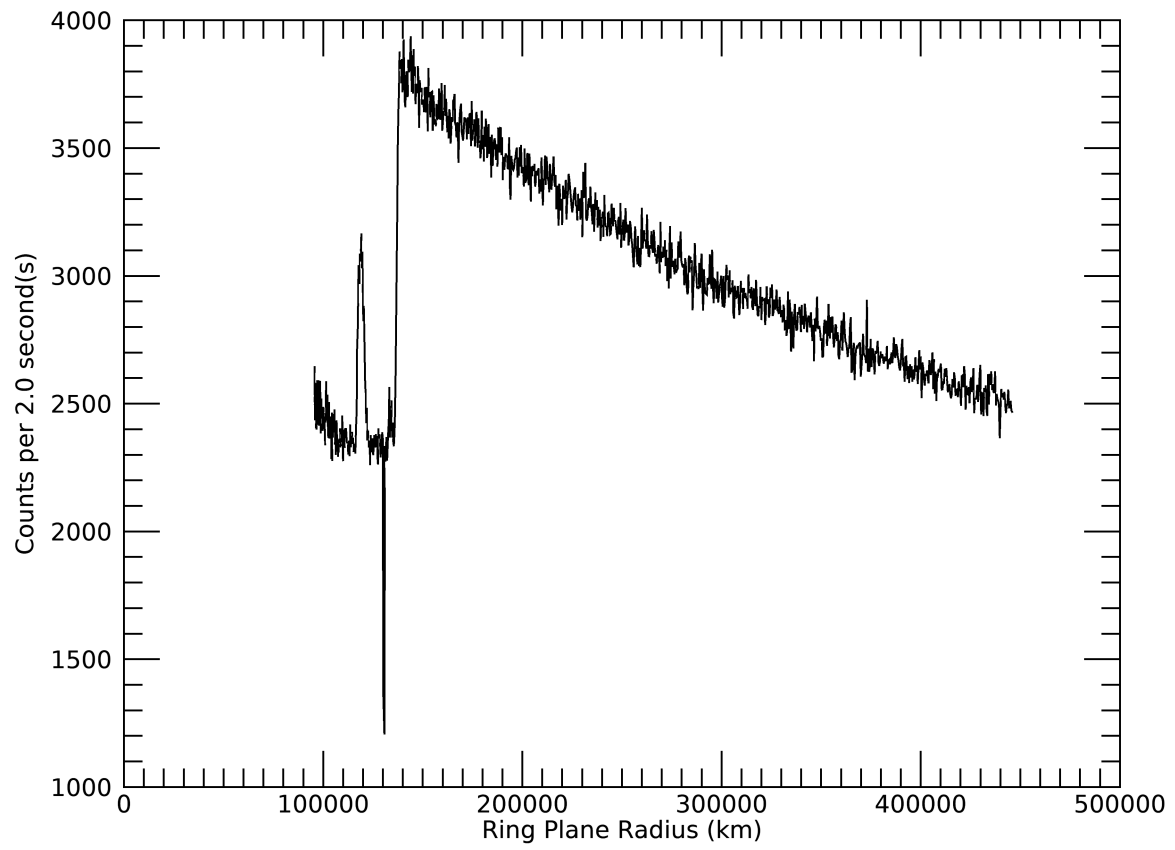
2008-121T10:10:00.000 276723.49 km

Target RA/dec: 322.48, -7.08

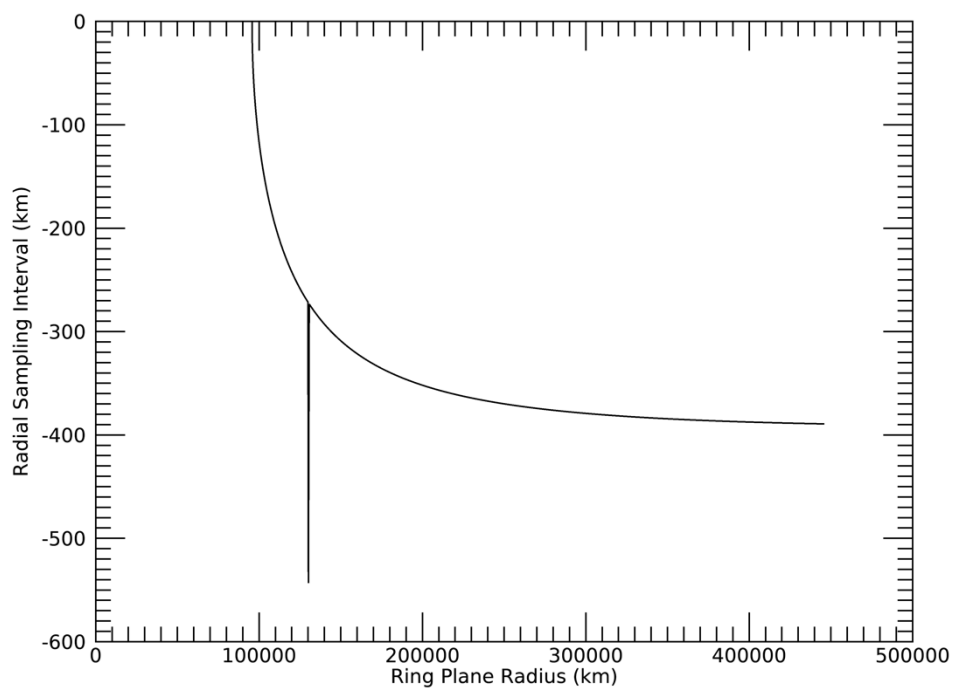
Subsolar lat/lon: -5.88, 157.39

Sub-s/c lat/lon: 4.84, -40.01

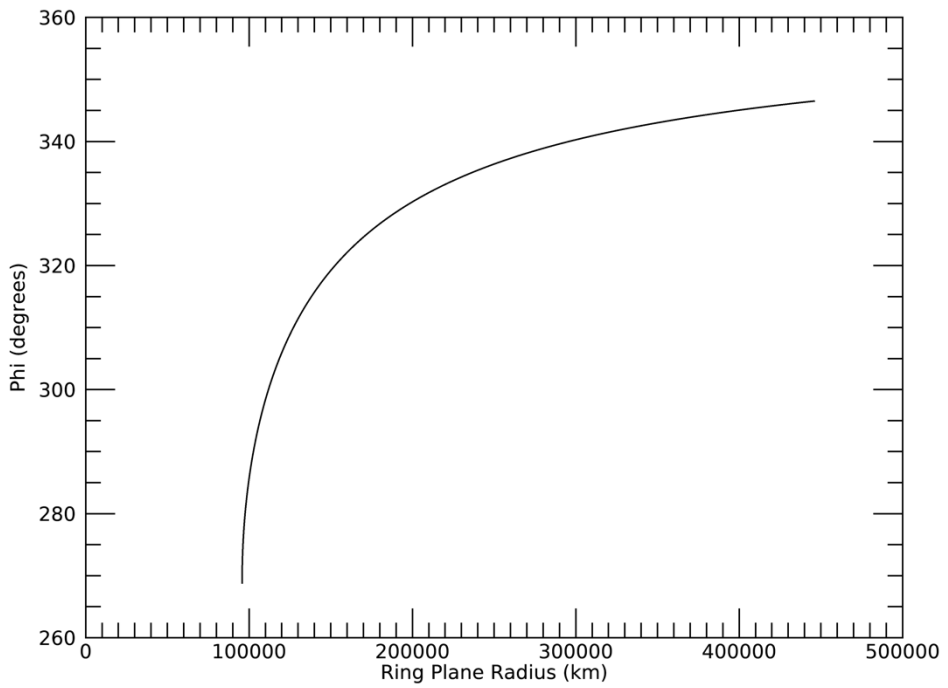
Rev 90I Signal

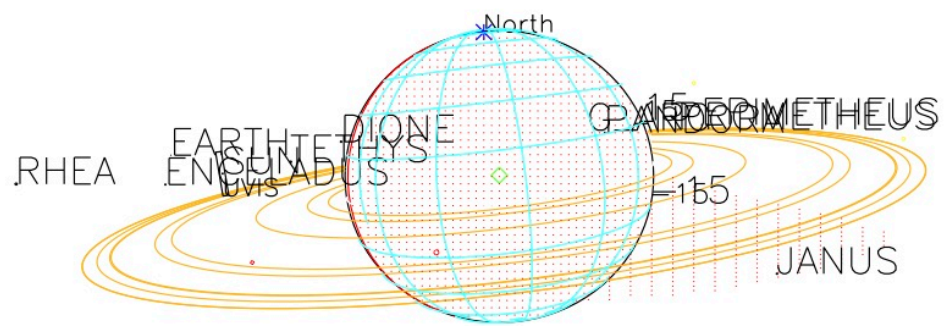


Rev 90I Radial Resolution



Rev 90I Phi





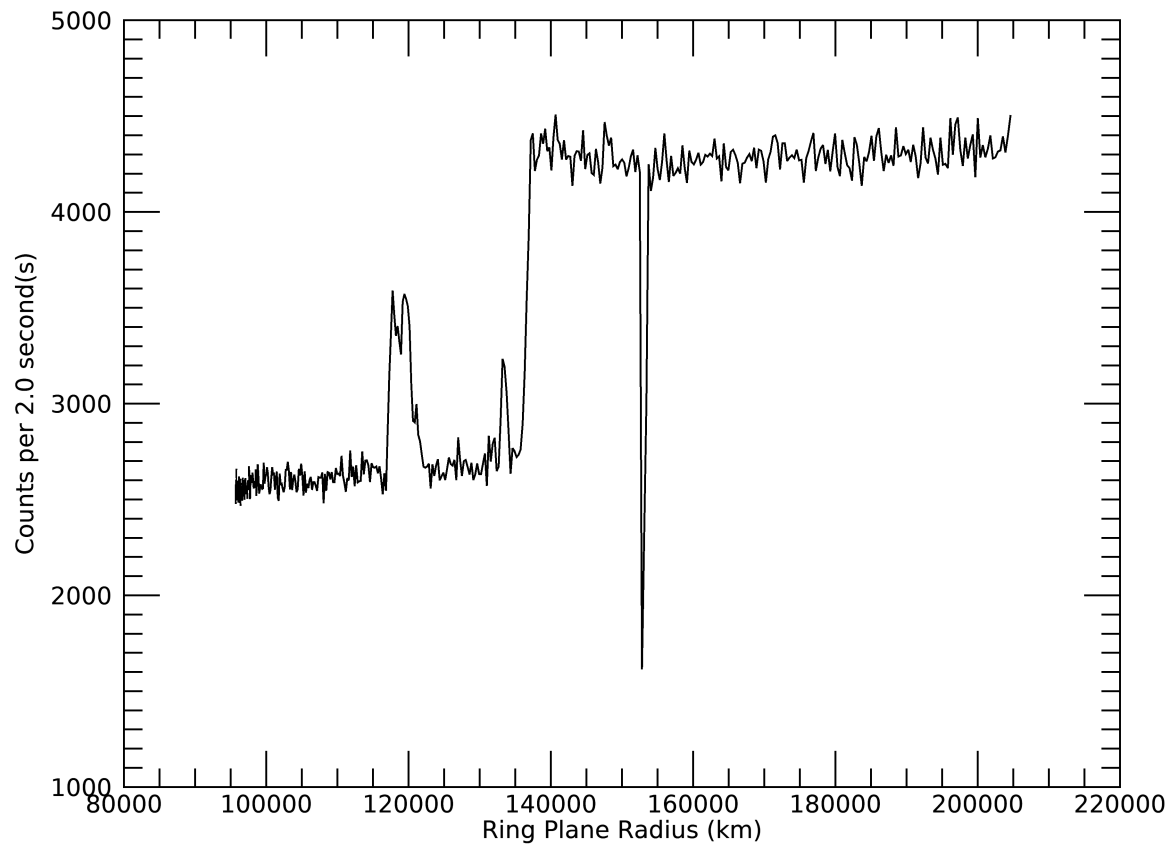
2008-298T09:28:00.000 242282.90 km

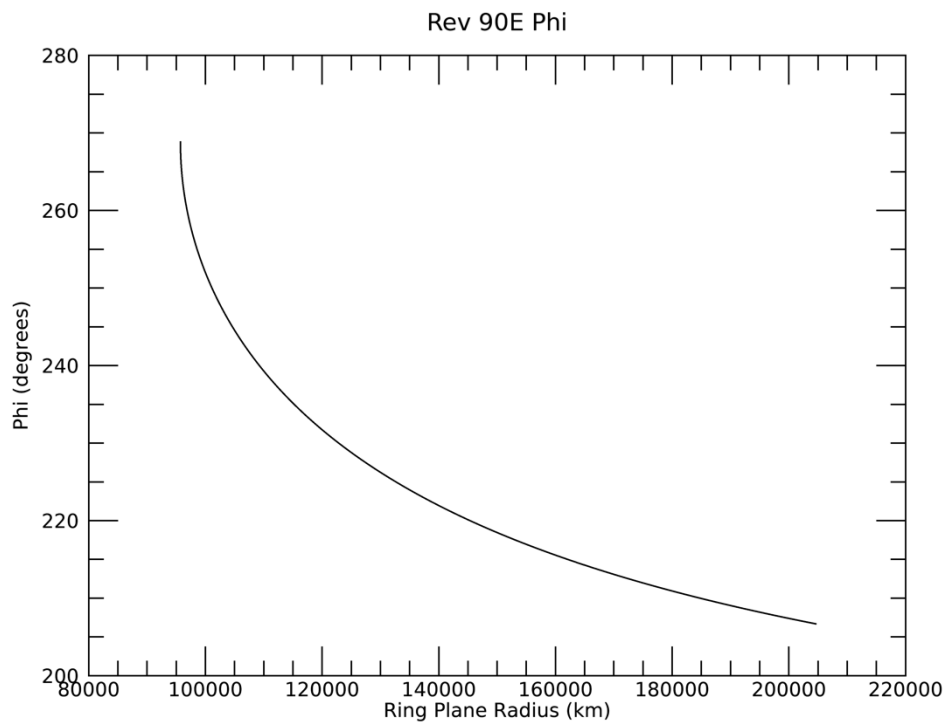
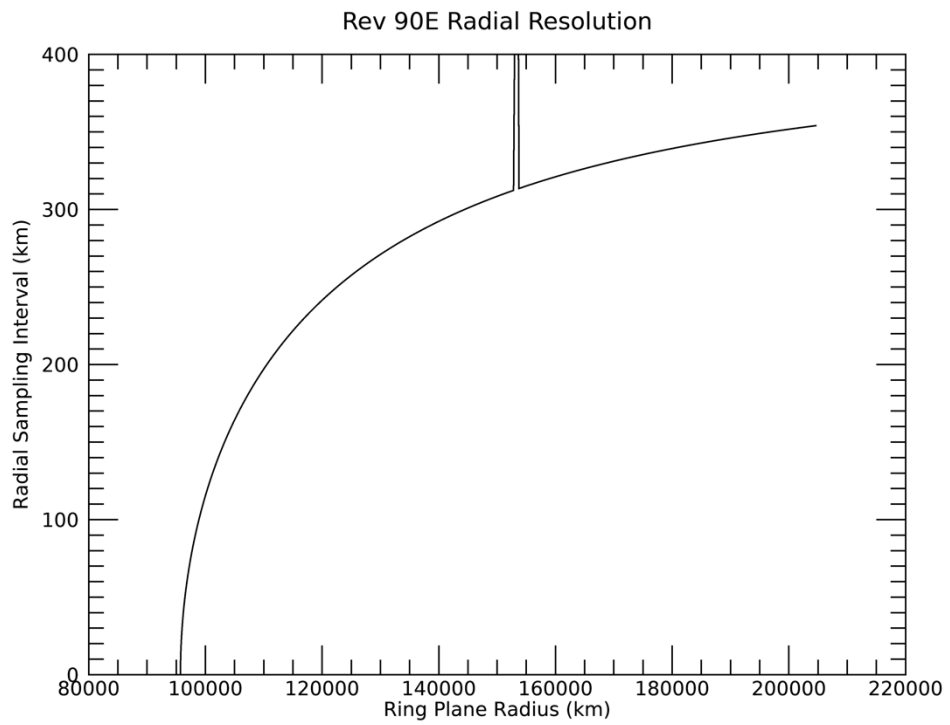
Target RA/dec: 320.58, -9.22

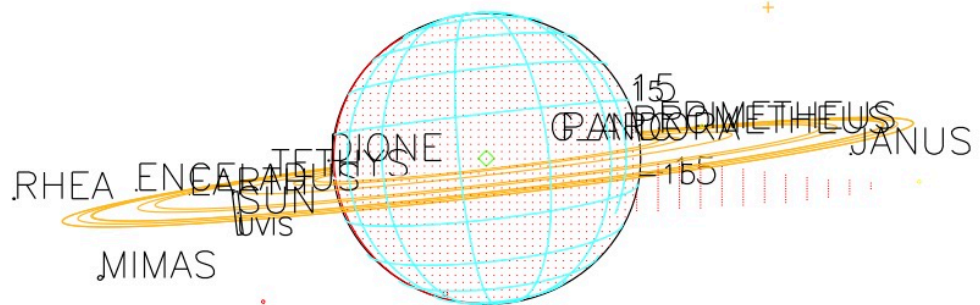
Subsolar lat/lon: -3.65, -43.90

Sub-s/c lat/lon: 6.87, 111.47

Rev 90E Signal







2008-298T09:53:00.000 239922.08 km

Target RA/dec: 322.75, -3.88

Subsolar lat/lon: -3.65, -57.97

Sub-s/c lat/lon: 2.13, 98.95